Available online at BCREC website: https://bcrec.id

Bulletin of Chemical Reaction Engineering & Catalysis, 17 (1) 2022, 163-193

Research Article

Layered Double Hydroxide Catalysts Preparation, Characterization and Applications for Process Development: An Environmentally Green Approach

Ateeq Rahman[1], Viswanadha Srirama Rajasekhar Pullabhotla[2,*]

[1]Department of Physics, Chemistry and Material Science, University of Namibia, Mandumedumefayo, Post Bag13301, Windhoek, Namibia.
[2]Department of Chemistry, University of Zululand, Private Bag X1001, KwaDlangezwa 3886, South Africa.

Received: 29th August 2021; Revised: 25th November 2021; Accepted: 26th November 2021
Available online: 23rd December 2021; Published regularly: March 2022

Abstract

The adage of new generation of fine chemicals process is the best process applied in the absence of conventional methods. However, many methods use different reaction parameters, such as basic and acidic catalysts, for example oxidation, reduction, bromination, water splitting, cyanohydrin, ethoxylation, syngas, aldol condensation, Michael addition, asymmetric ring opening of epoxides, epoxidation, Wittig and Heck reaction, asymmetric ester epoxidation of fatty acids, combustion of methane, NO_x reduction, biodiesel synthesis, propylene oxide polymerization. Layered Double Hydroxides (LDHs) have received considerable attention due their potential applications in flame retardant and has excellent medicinal property for reducing acidity. These catalysts are characterized using analytical techniques, such as: X-ray diffraction (XRD), Fourier-transform infrared (FT-IR), Raman spectroscopy, Thermogravimetric-Differential Thermal Analyzer (TG-DTA), Scanning electron microscope (SEM), Transmission electron microscopes (TEM), Brunauer-Emmett-Teller (BET) surface area, N_2 Adsorption-desorption, Temperature programmed reduction (TPR), X-ray photoelectrons spectroscopy (XPS), which gives its overall picture of its structure, porosity, morphology, thermal stability, reusability, and activity of catalysts. LDHs catalysts have proven to be economic and environmentally friendly. The above discussed applications make these catalysts unique from Green Chemistry point of view since they are reusable, and eco-friendly catalysts.

Keywords: Layered Double hydroxides; synthesis; applications; characterization; LDHs

How to Cite: A. Rahman, V.S.R. Pullabhotla (2022). Layered Double Hydroxide Catalysts Preparation, Characterization and Applications for Process Development: An Environmentally Green Approach. *Bulletin of Chemical Reaction Engineering & Catalysis*, 17(1), 163-193 (doi: 10.9767/bcrec.17.1.12195.163-193)

Permalink/DOI: https://doi.org/10.9767/bcrec.17.1.12195.163-193

1. Introduction

Anionic clay materials are a class of LDHs and the general formula of LDHs is $[M^{II}_{1-x}M^{III}_x(OH)_2]^{X+}[(Am^-)_{x/m}.nH_2O]X^+$, where $M^{(II)}$ and $M^{(III)}$ are the metal species being di- and tri- valents and A is an anion (Figure 1) [1]. LDHs are the host-guest materials consisting of positively charged metal oxide/hydroxide sheets with intercalated anions and water molecules [2]. There are enormous applications of LDHs catalysts, with few examples used as support for different catalytic materials [3–5] and as catalysts for organic transformations such as epoxidation reaction of olefins (styrene, cyclohexene) Mg-Al hydrotalcite [6], Aldol and Knoevenagel condensation Ni-Al hydrotalcite [7], Heck-

* Corresponding Author.
Email: PullabhotlaV@unizulu.ac.za (R.V.S.R. Pullabhotla);
Telp.: +27-35-902 6155

Suzuki reaction Mg Al-LDH-Pd° [8], hydroxylation of phenol, Michael reaction, transesterification CoNiAl hydrotalcite, LDHs as oxidation catalysts [9–11] and CO_2 absorbents [9], anion exchangers Ni-Al-LDH-Sn [10]. LDHs has vast applications in the area of environmental catalysis (Table 1), CuMgAl LDHs, which can be used in diesel engine soot [11–13], ion exchange/adsorption [14], drugs-Levodopa LDH nano composite shows minimal toxicity potential of a PC12 cell Parkinson's disease model in a dose [15], anti-cancer nano medicine [16], Lysozyme-LDH for antimicrobial activity [17], MgFe LDH-Mo can be used for degradation of methyl orange by photochemical method [18], Iron(III) Porphyrin MgAl LDHs [19,20], electroactive and photoactive materials MgAlCu Hydrotalcite [12], electrochemistry [21,22], fuel cell, and water splitting [22–26], LDHs carbon nano composites Ni/Co supercapacitors [27], Mg Al LDHs nano flakes humic acid adsorption [28], Biochar-Fe LDH for phenol removal [29], waste water treatment [30], LDHs nano carriers for drug delivery [31], LDHs based nano systems for cancer therapy [32], $NiCo_2S_4$@NiFe LDH hollow spheres as electrocatalysts [33]. Many reviews have been published focusing over particular examples, i.e. LDHs [34], LDHs hybrids [35], nanocarbons [36], Graphene LDHs nanocamposites [37], biomaterials-LDHs [38], LDHs preparation by continuous flow process [39], LDHS [40], LDHs present and future [41], synthesis characterization and applications [42], synthesis of new hydrotalcite type catalysts [43], intercalation method of organic molecules into LDHs [44], microwave-assisted synthesis on the physico-chemical properties of pamoate-intercalated layered double hydroxide [45], microwave hydrothermal treatments on the crystallinity properties of hydrotalcite-like compounds [46], microwave effect during aging on the porosity and basic properties of hydrotalcites [47], effect of synthesis conditions on the formation of layered double hydroxides [48], hierarchical nanocomposites derived from nanocarbons and layered double hydroxides, carbon nanoforms [49], metal nanoparticles [50,51], organic guests [52,53], and oxometallates [54,55] used for the preparation of interesting LDH-based hybrids, corrosion protection [56], anti corrosion [57], metallurgical application [58], Mg Al coatings on alloy [59], NiFeAl LDHs from electroplating sludge [60].

The concept of green chemistry is quite notable hence the authors presents the difference between conventional and green chemistry of heterogeneous catalysts in this section. The two key factors from Green chemistry point of view are (a) E-factor and (b) Atom economy. (a) E factor is defined as the mass ratio of waste to desired product formed. The E factor is the actual amount of waste produced in the process, defined as everything but the desired product. It takes the chemical yield into account which includes reagents, solvents losses, all process aids and, in principle, even fuel (although it is often difficult to quantify). A higher E factor means more waste generated and creating, greater negative environmental impact. The ideal E factor is zero. A very simple calculated outcome is quite simply, it is kilograms (of raw materials) in, minus kilograms of desired product formed, divided by kilograms of product out. (b) Atom economy is calculated by dividing the molecular weight of the desired product by the sum of the molecular weights of all substances produced in the stoichiometric equation. It is calculated by dividing the molecular

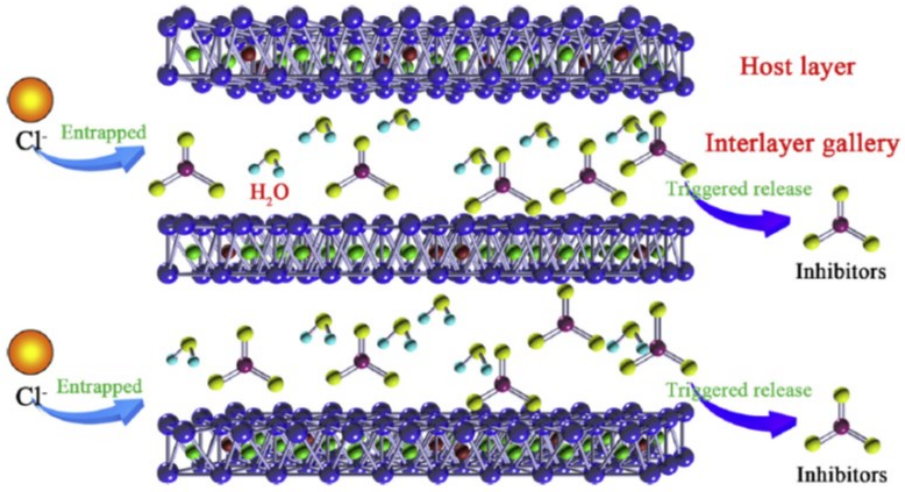

Figure 1. Schematic representation of the entrapment of the aggressive chloride ions and the triggered release of anionic corrosion inhibitors from LDHs [28].

Table 1. Applications of LDHs.

No.	Applications	Reference
1	Mg Al Hydrotalcite Epoxidation of olefins.	[6]
2	Aldol and Knoevenagel condensation Ni-Al hydrotalcite.	[7]
3	Heck-Suzuki reaction Mg Al-LDH-Pd^{o}.	[8]
4	Hydroxylation of phenol, Michael reaction, transesterification CoNiAl hydrotalcite, LDHs as oxidation catalysts.	[9–11]
5	CO_2 absorbents	[9]
6	Anion exchangers Ni-Al-LDH-Sn	[10]
7	Environmental catalysis Diesel Engine Soot.	[11–13]
8	Ion-exchange adsorption	[14]
9	Drugs-Levodopa LDH nano composite	[15]
10	Anticancer nano medicine	[16]
11	Lysozyme-LDHs for antimicrobial activity	[17]
12	Degradation of methyl orange with LDHs by photochemical reaction	[18]
13	Iron(III) Porphyrin MgAl LDHs.	[19,20]
14	Electroactive and photoactive materials MgAlCu Hydrotalcite	[12]
15	LDHs carbon nano composites Ni/Co supercapacitors.	[27]
16	Electrochemistry-Fuel cell and Water splitting.	[27]
17	Mg Al LDHs nano flakes humic acid adsorption	[28]
18	Biochar-Fe LDH for phenol removal	[29]
19	Waste water treatment	[30]
20	LDHs nano carriers for drug delivery	[31]
21	LDHs hybrids	[35]
22	Nanocarbons,	[36]
23	Graphene LDHs nanocomposites	[37]
24	Biomaterials-LDHs	[38]
25	LDHs preparation by continuous flow process,	[39]
26	LDHs present and future	[39-40]
27	Synthesis characterization and applications and Synthesis of new hydrotalcite type catalysts,	[42,43]
28	Intercalation method of organic molecules into LDHs.	[44]
29	Microwave assisted synthesis of LDHs	[45–49]
30	Hierarchical nanocomposites derived from nanocarbons and layered double hydroxides, carbon nanoforms	[50]
31	Metal nanoparticles	[50,51]
32	Organic Guests	[52,53]
33	Oxometallates	[54,55]
34	Corrosion protection	[56]
35	Anti-corrosion	[57]
36	Metallurgical application	[58]
37	Mg Al coatings on alloy	[59]
38	Ni Fe Al LDHs from electroplating sludge	[60]
39	Calcined hydrotalcites have been used for aldol	[61]
40	Knoevenagel and Claisen-Schmidt condensations.	[62]
41	Calcined hydrotalcites have been used for aldol, Knoevenagel and Claisen-Schmidt	[62]
42	Fe_3O_4/ZnCr LDHs nanohybrids Photo catalysts	[63]
43	SnO_2 Zr_2O_4 Photo catalysts	[64]
44	MgZn LDHs Photo catalysts	[65]

weight of the product by the sum total of the molecular weights of all substances formed in the stoichiometric equation for the reaction involved. The conventional processes produce copious amounts of inorganic salts can similarly be largely replaced with stoichiometric mineral acids, such as H_2SO_4, and Lewis acids and stoichiometric bases, such as NaOH, KOH, and NaOMe with recyclable solid bases, in a variety of organic transformations it is a focus of recent attention [66] preferably in catalytic amounts. However, the technology has not changed for a century replacing the traditional processes with the heterogeneous catalysts, such as synthetic hydrotalcite clays which are also known as layered double hydroxides (LDHs) are examples. Calcined hydrotalcites have been used for aldol [61], Knoevenagel [62], and Claisen-Schmidt [62] condensations to name few (Table 1). Hence due to the toxic waste produced heterogeneous catalysts can minimize toxic waste with concept of green chemistry.

The LDHs has Green chemistry concept that promotes environmental and development of sustainable technologies. LDHs is one of the key technologies on which new approaches to green chemistry are based. Green catalysis recently made significant progress in several areas such as the design of safer chemicals and environmentally benign solvents, and the development of renewable feedstocks, such as biomass. In a nut shell, it is necessary to design LDHs catalysts and catalytic processes with in order to follow the environmental regulations.

2. Crystal Structure of Hydrotalcite

LDHs structural role remains to reconstruct the lamellae to establish the electro-neutrality throughout the linkage; where water molecules are distributed. LDHs structures are usually derived from mineral brucite, $Mg(OH)_2$. Mg ions are present in $Mg(OH)_2$. In octahedral sites Mg ions are situated with six OH− groups pointing at the vertices, whereas they are pointing the H atoms in the path of the interlayer spacing. Hence, the octahedral sites are interconnected together by boundaries creating the planar and neutral extended layers interconnected with H bonds. The crystal structure can have rhombohedral of hexagonal symmetry. The bivalent cations are moderately exchanged with trivalent ones, and the positively charged sheets are formed. In brucite layers the electrostatic interactions takes place with hydrogen bonds, this controls the resulting arrangement of the layers. The crystal structure arising from the stacking of sheets could be rhombohedra or hexagonal symmetry. However, maximum number of synthetic LDHs exhibits rhombohedral R-3 unit cell. A very important criterion for the LDHs stability exhibits due to the cations situated in the octahedral sites and must possess similar ionic radii. However, the ratio of M^{2+}/M^{3+} is between 1–3. Hence, in principle, there are no restrictions for the anionic species that balances the positive residual charges [65].

3. Methods for Preparation of LDHs

The most common methods for the synthesis of LDHs are discussed below.

3.1 Mechanochemical Method

This method has been effectively used for the intercalation purposes. A simple method is used by grinding with mortar and pestle and it is similar to anion exchange method. The prepared NO_3^- ion containing LDHs was used as a precursor material and anion is added with a very minute amount of NaOH and grounded manually. During grinding process, the NO_3^- ions with desired molecules are in anionic form [67].

3.2 Liquid Assisted Grinding Method

The MgAl-NO_3 with the formula $Mg_{0.63}Al_{0.37}(OH)_2$ $Al(NO_3)_{0.37}.0.4H_2O$ was prepared using the urea method [67] which resulted in the formation of Mg Al carbonate hydrotalcite. Instantaneously, it was converted into its nitrate form by titration. It was then dispersed in a $NaNO_3$ solution (mol/L) and titrated by a HNO_3 solution (0.1 mol/L) by means of an automatic titrator (I tralab VIT 90 Video Titrator Radiometer, Copenhagen) operated at pH Stat mode at pH 5.

3.3 LDHs Synthesis using Microwave

The ageing process takes place in microwave conditions, however the irradiation of the microwave is taken into consideration where very fast ageing process takes place, for about 15–60 min [68]. The co-precipitation and urea techniques can be utilized as a part of a synthesis using microwave [69] rather than a reflux aging process. Homogeneous sized particles are synthesized using microwave aging process, that are in smaller size than nano particles produced using reflux method [69]. The main advantage of shorter duration of aging process is to prevent the formation of impurities. However, with long duration of time for the aging process changes the formation of impurities which are quite high. Choudhary *et al.*

[70,71] reported that the Ni Al hydrotalcite is effective for oxidation and reduction reactions as NiO in association with oxide of aluminium from TPR studies. Kantam *et al*. [72] reported that the $MgAlCO_3$ hydrotalcite hence the carbonate is favouring ring opening of epoxides.

3.4 Co-precipitation Method

This is a commonly and economic method used to prepare LDHs since it is usually prepared in a solitary step with a good yield [72]. The M^{2+} and M^{3+} solutions of cations are stirred together with another solution of anion to be intercalated, under constant stirring at room temperature. Hence, the pH of the mixture is maintained at 9 by addition of basic solution of sodium hydroxide and sodium carbonate of known concentration to favour the precipitation of cation hydroxides. To support the intercalation of the preferred anions, the ideal ions of cation salts are nitrates or chlorides that has low affinity on the brucite layers. Hence, the absence of CO_2 in water is crucial for the preparation of intercalated LDHs. A vital measure is to be adopted with the use of de-ionized water in an inert atmosphere, this is to avoid the interaction of the solution with air/moisture. The impurity phase formation is determined with the perfect choice of pH value, and depends on the cations ratio. The crystallinity of the resulting LDHs nano hybrids slowly increases for six hours at 80 °C. From literature it is evident that, there are many examples of this methods that are reported for the synthesis of nanocomposites which are used for drug delivery, intercalation of drugs, anticancer agents [73], pesticides [74], amino acids [75], peptides, and antibiotics [76].

3.5 Hydrothermal Synthesis Method

The hydrothermal synthesis usually begins with fast mixing of oxides/hydroxides of M^{2+} and M^{3+} cations. The solution of desired acid or salt is introduced into the suspension, then the obtained dispersed solution is stirred at high temperature in 3-neck round bottom flask or in hydrothermal reactor. The advantages of this method is to minimize the formation of undesirable waste, which causes pollution to the environment. Additionally, since only metal hydroxides, shows very short affinity towards LDH interlayers that are existing. However, the hydrothermal method is very effective in intercalating the organic guest species between the LDH interlayers. This method is very important to control and achieve the desired particle size and morphology which usually depends on parameters set. In many developmental processes, this method is utilized to improve the crystalline structure of LDHs for exhibiting excellent properties [76].

3.6 Synthesis of LDHs by Sol-gel Method

LDHs are prepared by Sol-gel process, the mechanism shows the formation of sol during hydrolysis and the partial condensation of a metallic solution which is the first step, and the second step is followed by gel formation. Hence, metallic alkoxides, acetates, or acetyl acetonates, and inorganic salts are used as metallic precursors. The interesting properties of the resulting solid LDHs depends on certain defined parameters, such as hydrolysis and slow condensation of metallic precursors, that are finely tuned by regulating different reaction parameters adopted such as pH, concentration of the metallic precursors, solvent and temperature. The materials synthesized by Sol-gel method shows pore sizes that are well controlled and has high specific surface area as reported by Yang *et al*. [77].

3.7 Reconstruction Method

This is the most important and interesting method which has advantages of the 'memory effect' of LDHs. In detail, these materials, once heated at elevated temperatures of about 650 °C in inert conditions, results in the formation of mixture of metal oxides that are easy to regenerate the hydroxide layers when exposed to water. These are highly applicable in base catalysed reactions such as Aldol, Michael, and Wittig reactions [78]. The prepared LDH-CO3 are thermally decomposed to a mixture of oxides which is easily dispersed in the desired anion solution under inert conditions in deionised water in order to avoid the CO_3^{2-} contamination. This is the common method used when larger anions have to be intercalated in LDHs. Hence, this method is the choice of method for intercalation, with different anions, such as Cl^- or NO_3^- [78]. The incorporation of competing anions is also restricted, depending on parameters such as pH value which increases leading to favour the OH^- formation. Various examples have been reported in literature, such as pesticides, vitamins and antibiotics [79].

3.8 Ionic Exchange Method

Ion exchange and co-precipitation are complementary methods. In precise, the selected metal ions which are at high pH and/or when there is a robust prospect of interaction

amongst guest species and metal ions, they are typically seen as unstable [79]. With the anion-exchange process, the LDHs structure usually contains Cl^- or NO_3^- as interlayer anions, that are added to the concentrated solution of the anions. The resulting solution is stirred overnight at temperature range of 50–70 °C. The exchange efficiency differs usually depends on the capability of the exchanged anions to stabilize the layered structure. However, the two steps discussed above are very important, but many examples are cited in literature in drugs [79], and pesticides [79] intercalations.

3.9 LDH Synthesized in T-Mixer with Ultrasonic Process

A mixture of 0.03 mol L1 $Mg(NO_3)_2$ and 0.01 mol L1 $Al(NO_3)_3$ and solution NH_3H_2O (100 mL) with certain concentration was simultaneously transported into a 'T-type' impinging-stream reactor by means of metering pumps at the rate of 100 rpm to produce MgAl LDHs. Ultrasonic processing was also applied during this process and the frequency was kept at 20 kHz. The pH of the whole solution was continuously kept at 10 through regulating the concentration of NH_3H_2O. The resulting mixture was washed with water several times until it recached pH = 7 and then it was dried at 100 °C in an oven. The resulting material was denoted as "T-mixer", TU-LDHs [80].

3.10 LDH Synthesized by Hybrid Two-step Method

MgAl layered double hydroxides were prepared using a hybrid two-step preparation approach. The hybrid two-step preparation comprises of the mother solution prepared in 'T-mixer' accompanying with ultrasonic processing (first step) and the following step of co-precipitation (second step) process. The mother solution was synthesized according to the preparation method of the Section 3.9. About 50 mL of the mother solution from Section 3.9 which was added into a beaker for continuous stirring. Then, 150 mL of salt solution with a fixed concentration of 0.03 mol/L $Mg(NO_3)_2$, 0.01 mol/L $Al(NO_3)_3$ and 1 mol/L of NH_3H_2O were simultaneously added to the mixture at the second step. The addition rate of salt solution was controlled by regulating the speed of peristaltic pump, where the pH of the whole solution was continuously kept at 10. The final obtained materials were filtered and then washed with distilled water until pH = 7 was reached, then followed by drying at 100 °C in an oven. The obtained material was denoted as "T-Mixer "TUC-LDHs [80].

4. Characterization of LDHs Catalysts

LDHs are usually characterized by X-ray diffraction (XRD), Differential Scanning Calorimetry-Temperature Gravimetric Analysis (DSC-TGA), Fourier Transform Infra Red (FT-IR), X-ray Photoelectron Spectroscopy (XPS), Raman, Temperature Programmed Reduction (TPR), and Scanning Electron Microscopy (SEM) spectroscopy.

4.1 SEM Characterization of CoAl LDHs

SEM analysis is a powerful investigative tool which used to characterize which produces high magnification images of a sample's surface. Basically in LDHs samples they are highly crystalline. Intersected, nearly hexagonal-shaped particles, interconnected with each other, enough uniform as sizes (average size equal to 100 nm) are formed in the case of the hydrotalcite-like clay Mg Al LDH. Bayu [81] reported that Mg Al (2:1 and 3:1) prepared by co-precipitation method showed morphology of thin crystals of nanoparticles of agglomerates of Mg-Al hydrotalcites [81]. Wu *et al.* [82] reported the characteristic SEM morphologies of LDHs samples. The morphology of Co-Al LDHs synthesized at 80 °C is different from that of synthesized at 140 °C, and the crystallization temperature on the morphology of LDHs. The LDHs at low crystallinity were assembled to observe as a single layer. Wu *et al.* [82] reported that the morphologies of LDHs were further confirmed with TEM as micro morphologies, and the LDHs were formed as hexagonal layered structures. In addition, the agglomeration of particles was observed in LDHs samples that resulted due to the physical entanglement of organic anions. Zhai *et al.* [83] reported the agglomerated layers of Co-Al LDHs samples through SEM analysis, the samples were prepared at 80 °C. These SEM results revealed the morphology of Co-Al LDHs which shows interesting properties such as high chemical and thermal stability, intercalated anions with interlayer spaces, ease of synthesis, unique structure, uniform distribution of different metal cations in the brucite layer, surface hydroxyl groups, flexible tenability, Oxo bridged linkage, swelling properties and ability to intercalate different type of anions, such as oxalate, *t*-K-But oxide, LDA-Lithium di-isopropyl amide [84].

4.2 XPS Characterization of LDHs:

X-ray photoelectron spectroscopy (XPS) is very important tool to detect the chemical composition and evaluate the chemical bonding states (or oxidation state) as well as the electronic structure of the surface. Nishesh [85] reported the chemical composition determined by the full XPS spectrum of Zn–Fe LDH which showed the presence of C, O, N, Fe, and Zn. The presence of carbon is due to carbonated anions in the LDH material. The high-resolution XPS (HRXPS) spectrum of O 1s deconvoluted into three peaks where binding energy at 528.41 eV and 530.07 eV were ascribed due to the lattice oxygen (O_2^{2-}) and surface hydroxyl groups of metal centers, respectively. The broad peak at 530.94 eV corresponds to the physisorbed/chemisorbed water molecules, carbonate, and nitrate ions [85]. The Fe 2p3/2 peak at 710.74 eV and Fe 2p1/2 peak at 724.16 eV along with satellite peaks at 717.82 eV (2p3/2) and 733.04 (2p1/2) related to the existence of Fe^{3+} oxidation state [85]. Two noticeable spin-orbit peaks observed at 1020.30 eV and 1043.53 eV were due to Zn^{2+} [85]. Fe and Zn were distributed homogeneously in the material. Where the surface Zn/Fe ratio was 1.9. The XPS results together with the LDHs was reported by Karolina [86]. However, in order to characterize the nature of interlayer anion and structural changes in the reference samples along with increasing molar ratio, the XPS analysis of C1s and Mg1s was performed for the reference samples, as well as their analogues derived from minerals. The XPS analysis penetration depth was approximately 9 nm. The C1s peaks exhibited two maxima which is ascribed due to the organic carbon contamination (~285 eV) and carbonates (~290 eV). The C content in all samples was equal to ~2.0 %wt. which is consistent with the results of elemental analysis. Peaks fitting revealed components assigned to: CC (284.8 eV); C−O−C (286 eV); C=O (286.6 eV); O−C=O (287.5 eV); CO_3^{2-} (289 eV) and HCO_3^- (290 eV) [86].

4.3 FT-IR Characterization of CoAl LDHs

FTIR Spectroscopy, is a vital analytical technique used to identify organic, polymeric, and, in some cases, inorganic materials ans study its functional group's. The FTIR spectra of the LDHs reveals bands that are characteristics of hydrotalcite-like compounds. The broad and strong band centred at 3400 cm^{-1} is ascribed due to the stretching of the OH bond of the hydroxyl groups and interlayer of H_2O molecules in LDHs samples [87]. The shoulder around 3050 cm^{-1} is ascribed due to the $H_2O{-}CO_3^{2-}$ interlayer bridging mode by hydrogen bonds [87]. The weak band at 1630 cm^{-1} is attributed due to the H_2O bending deformation located in interlayer spacing on the LDHs. The sharp, intense vibration bands observed around 1370–1380 cm^{-1} were designated to the asymmetric stretching of CO_3^{2-} anions. This band is broad, which is ascribed due to the presence of nitrate ions from the starting salts, principally due to the mode of vibration of NO_3^- is generally overlapped by the mode of vibration of CO_3^{2-} [87]. The bands are recognized at 460, 550, and 790 cm^{-1} are credited to the Al−O condensed groups, the Zn/Al-OH translation and the Al−OH deformation, correspondingly. For example the Zn-Al-CO_3 sample, the band around 1365 cm^{-1} is due to the antisymmetric stretching mode of carbonate, and bands observed around 870 and 680 cm^{-1} are ascribed due to the weak non-planar bending mode and the angular bending mode of carbonate present in the interlayer of LDH. The FTIR spectra of Zn-Al-NO_3 reveals a strong peak around 1380 cm^{-1} and is endorsed due to the antisymmetric stretching mode of the nitrate anion present in the LDHs [87]. The bands recorded around 839 and 670 cm^{-1} are ascribed due to the weak out-of-plane symmetric deformation mode and the anti-symmetric deformation mode of nitrate, correspondingly [87].

4.4 Raman Spectra Characterization of LDHs

Raman spectroscopy is a spectroscopic method used to detect vibrational, rotational, and other states in a molecular system, capable of probing the chemical composition of materials. Luiz [88] reported that the Raman spectra shows bands in the region of 470 cm^{-1} which is ascribed due to the vibration connections of Al−O−Al present in the layers of Mg-Al-LDHs sample. Nishesh [85] reported the Raman spectra of pristine, P-adsorbed (pH 8), P-adsorbed (pH 5), and P-desorbed Zn–Fe LDH. The Raman analysis of phosphate adsorbed Zn–Fe LDH at pH 5 and at pH 8 revealed significant fluctuations in the peak position and intensity a compared with the pristine LDH [88]. At pH 5, signal intensities for M−O−M vibration peaks were low compared to the pristine form and was due to the deterioration in the structure of LDH. At pH 8, the Raman spectrum was found like that of the pristine LDH. An increase in the intensity of band centered at 1104 cm^{-1} was attributed due to the peaks of adsorbed PO_4^{3-} which appears in the range of

900–1200 cm^{-1} and thus broadened the band [88]. The Raman spectra shows a sharp band at 1064 cm^{-1} which indicates the symmetric C–O stretching vibrations of carbonates/bicarbonates in the interlayer space of LDH reference samples, followed by bands of low intensity at 986 and 688 cm^{-1} confirms the presence of bicarbonates in the Mg/Al LDH samples with high molar ratio [88]. However, the intensive, sharp bands at ~670 cm^{-1} were observed for the Mg/FeLDH samples. Broadbands at ~1600 cm^{-1} and 1330 cm^{-1} were ascribed due to the carbonates in the Mg/Al and Mg/Fe LDH samples, respectively. It is worth to mention that the bands related to carbonates in the Mg/Fe LDH samples had a high intensity and indicated a different nature of interlayer anions in comparison to the Mg/Al LDH samples.

4.5 DTA-TGA Characterization of Zn-Al LDHs Catalysts

The DTA-TGA Technique Characterizes materials by Measuring Changes in Mass as a function of Temperature. Thermogravimetric analysis (TGA) is widely used in materials science stream together with DSC, TMA, and DMA. TGA measures the mass of a sample while the sample is heated or cooled in different atmosphere. The DTA-TGA analysis of Zn-Al LDHs was characterized in order to evaluate the disappearance of H_2O molecules, and other intercalated groups such CO_3, NO_3, SO_4^{2-} an anionic groups when heated at high temperatures [89]. It was observed that the weight loss was due to the incorporated molecule which had been burnt. The thermogravimetric analysis of the synthesized LDHs shows that the TGA-DTA patterns were characterized by a weight loss between 10 and 14% due to the loss of the interlayer water in the temperature range of 50–250 °C. For Zn–Al–CO_3 there are two steps that takes place during dehydration at 150 °C and 250 °C. These steps are due to the loss of adsorbed and interlayer water followed by water loosely coordinated to the interlayer carbonate. However, the interlayer carbonate is released as CO_2 at approximately 350 °C. The total mass loss was 20.86%. For Zn–Al–NO_3, there are mass losses at 150, 250, 350 and 450 °C. The mass losses at 150 and 250 are escorted by a change in the heat flow; it was resulted from the removal of the adsorbed surface water and the interlayer water [89]. The second distinct mass loss in the temperature range of 350–460 °C results from two steps, such as the dehydroxylation of the Zn–Al–LDH layers and the decomposition of the interlayer NO_3^- anions. The total mass loss were around 21.5%. TGA-DTA analysis for Zn–Al–Cl LDHs shows similar dehydration behaviour compared with Zn–Al–NO_3, but Cl was lost in the temperature range of 400–500 °C. The total mass loss at 700 °C was 18.84%. The decomposition of Zn–Al–SO_4 occurred in the following steps: the first mass loss at 150 °C matched to the evaporation of surface-adsorbed water followed by evaporation of the interlayer water at 250 °C; a third loss of mass occurring at 350 °C was ascribed due to the dehydroxylation of the brucite-like octahedral layers. The fourth step at 600 °C was likely due to the elimination of the intercalated SO_4^{2-} in the Zn–Al LDH interlayers [89]. DTA-TGA analysis shows whether the anions are decomposed in the interlayer of LDHs.

4.6 XRD Characterization of LDHs

XRD is an instrument is used to characterize the nature of the LDHs such as crystalline or amorphous. The XRD analysis is done with an X-ray source of Cu-K_α radiation (λ = 1.5406 Å). It will analyze and identify the unknown crystalline compounds by Brag Brentano method. The diffractogram of the precursor material (Mg_2AlCO_3-LDH) shows both sharp and symmetrical peaks and some high angle asymmetrical peaks; this provides proof of well crystallized and ordered layered structure of Mg_2AlCO_3-LDH. The characteristic pattern of hydrotalcite is present, to be precise a set of four reflection lines at 2θ = 10, 20.00, 38.56 and 61.00° were due to the reflections of the sharp and basal planes corresponding to the (003), (006), and (009). With broad reflections for (015) and broad reflections for (110) are defined due to the crystalline patterns respectively. The XRD reflections for LDH samples are usually indexed using a hexagonal cell with rhombohedral symmetry R −3 m. Said *et al.* [90] reported that the for Mg-Al CO_3 HT calcined samples at 450 °C, the X-ray patterns of the calcined materials, observed two new intensive diffractions lines at around 43.1 and 62.5°, which correspond to the (200) and (220) reflections of the MgO periclase-type structure [90]. Diffraction peaks of brucite matched with a standard pattern (JPCDS No. 98-003-4961) [91]. The (003) sharp intense strong peak were attributed due to the crystallinity of LDHs formed, and the remaining peaks were not intense this could be due to the PH parameter during the synthesis of LDH. The Mg_2AlCO_3-LDH spacing (that is, the thickness of a layer

plus the interlayer space) is 8.77 Å, value greater than that of a hydrotalcite of this type which is normally 7. 65 Å [91]. XRD of MMgAlO reported by Marcu *et al.* [92] that the MMgAlO samples calcined at 550 °C displayed, in all the cases, the same peaks at 2θ 43.5 and 63° than the MgAlO mixed oxide which corresponded to the (200) and (220) reflections of the periclase-like structure (JCPDSICDD 4-0829). However, weak reflections that can correspond to both Fe_2O_3 (JCPDS 39-1346) and $FeAl_2O_4$ (JCPDS 34-0192) phases whose peaks are superimposed, were observed for FeMgAlO catalyst. No segregated phases were observed in the other samples suggesting that the mixed oxides were solid solutions containing the transition metal cations [92].

4.7 BET Surface Area of LDHs

Brunauer–Emmett–Teller (BET) theory aims to explain the physical adsorption of gas molecules on a solid surface and serves as the basis for an important analysis technique for the measurement of the specific surface area of materials. The observations are very often referred to as physical adsorption or physisorption. The surface area (S_{BET}) of the samples were determined using BET (Brunauer, Emmett and Teller) model. The total volumes were calculated according to the amount of nitrogen (N_2) absorbed at a relative pressure (P/P_O) of 0.99. The pore volumes were calculated from the desorption branch of the isotherms using the Barrett-Joyner-Halenda (BJH) method, for the pores between 1.7 and 300.0 nm. It was clearly observed that the S_{BET} of (TUC-LDHs) is the highest of 235.3 m^2/g compared to 198.7 m^2/g for "T-mixer" (TU-LDHs) and 148.1 m^2/g for CC-LDHs as well as the pore sizes (90.83 Å) and highest pore volume (0.48 cm^3/g). Both of "T-mixer" Pretreatment followed by conventional co-precipitation (TUC-LDHs) and Conventional coprecipitation (CC-LDHs) facilitates the macrostructure of pores. However, the TU-LDHs has the second largest S_{BET}, its pore sizes (24.4 Å) and pore volume (0.08 cm^3/g) are the lowest in comparison with other two materials. This indicates that the TU method contributes to the formation of mesoporous structure.

The increase in surface area of TU-LDHs is likely caused by the enhanced micromixing in the 'T-mixer', where the use of ultrasonication can intensify the turbulent eddies and those microbubble bursting that erode the surface area of layered structure through removal of the interlayer anions [93]. Said *et al.* [94] reported that the Mg Al Ht carbonate shows BET surface area of $Mg_2Al–CO_3$ HT-75 $Mg_{2.5}Al–CO_3$ HT-93, $Mg_{3.0}Al–CO_3$ HT-105, $Mg_{3.5}Al–CO_3$-101 HT, $Mg_{4.0}Al–CO_3$ HT-56, from these surface it is evident that on calcination, the disappearance of water and carbonates leads to a considerable increase in the surface area and volume of the pores ranging from 0.33-0.61 [94].

4.8 N_2-Adsorption-desorption of MgAl LDHs

A plot of relative pressure vs volume adsorbed obtained by measuring the amount of N_2 gas that adsorbs onto the surface of catalysts *i.e.* sorbate, and the subsequent amount that desorbs at a constant temperature. N_2 adsorption-desorption isotherm of MgAl LDHs for all the adsorbents show a Type IV isotherm according to the IUPAC classification, which is connected with mesoporous materials [95]. TUC-LDHs and CC-LDHs shows a H3 type hysteresis loop, signifying that the pores are produced by 'slit-shaped' of plate-like particles [95]. This type of isotherm is generally observed in the mesoporous stacking structure of sheet-like 2D crystallites [95]. In the case of TU-LDHs, it shows a H2 type hysteresis loop corresponding to a complex and interconnected pore structure, indicating that the pores are produced by rapid nucleation process.

The surface area (S_{BET}) of the samples were determined using BET (Brunauer, Emmett and Teller) model. The total volumes (V Total) were calculated according to the amount of nitrogen (N_2) absorbed at a relative pressure (P/P_O) of 0.99. The pore volumes were calculated from the desorption branch of the isotherms using the Barrett-Joyner-Halenda (BJH) method, for the pores between 1.7 and 300.0 nm. It was observed clearly that the S_{BET} of "T-mixer Pretreatment followed by conventional coprecpitation (TUC-LDHs) is the highest of 235.3 m^2/g compared to 198.7 m^2/g for TU-LDHs and 148.1 m^2/g for conventional coprecipitation (CC-LDHs) as well as the pore sizes (90.83 Å) and highest pore volume (0.48 cm^3/g). Both of TUC-LDHs and CC-LDHs facilitate the macrostructure of pores. However, "T-mixer" TU-LDHs has the second largest S_{BET}, its pore sizes (24.4 Å) and pore volume (0.08 cm^3/g) are the lowest in contrast with other two materials. This attributes that the TU method contributes to the formation of mesoporous structure. The increased micromixing in the 'T-mixer' could possibly cause the increased surface area of TU-LDHs. Here, ultrasonication can multiply the turbulent eddies and microbubble bursting erodes the surface area of hydrotalcites of layered structure while the in-

terlayer anions are removed [95]. However, during the calcination, the departure of water and carbonates leads to a considerable increase in the surface and volume of the pores [96].

4.9 TPR Characterization of Mg Al LDHs

Temperature Programmed Reduction (TPR) is a characterization of materials generally used in catalysis studies to characterize the surface chemistry of metals and metal oxides under varying thermal conditions. TPR-enabled mass spectrometry equipment can acquire quantitative and qualitative data relating to the reducing gas mixtures that are made to flow over metallic samples. Ibrahim [97] reported the TPR characterization of MgAl LDHs catalysts of three samples. The peaks shifted towards lower time when the Mg content is higher. Although, the amounts of consumed H_2 decreased with the increase in Mg content which are 3175.91765, 1395.65979, and 277.55466 mol/g, respectively. The amount of gas uptake were very little as MgO is difficult to be reduced. Hence, for calcined Mg-Al HTlcs or MgO, no reduction peaks were detected until 900 °C. Saikia [98] reported that the metal-support interaction is another factor affecting the catalytic performance, of Ru-Mg Al LDHs catalysts which was analysed by H_2-TPR. However, for the control experiment using the commercial RuO_2 catalyst, only one reduction peak at 213 °C was observed, corresponding to the reduction of Ru^{4+} to Ru°. However, the 2.5% Ru/MgAl catalysts, TPR results indicated that, in general, the metal-support interaction becomes stronger with an increase in the reduction temperature.

In the case of the as prepared $RuCl_3$/MgAl LDH, the peak at 126 °C can be assigned for the reduction of $RuCl_3$ adsorbed on the surface of MgAl LDH [98]. For the reduced 2.5% Ru/MgAl catalysts, three reduction peaks centred at 120−180 °C (peak I), 185−220 °C (peak II), and 320−340 °C (peak III), which was ascribed due to the weakly supported RuOx species on the support, strongly supported RuOx species and the surface or subsurface oxygens, respectively [98]. With 2.5% Ru/MgAl catalysts was reduced at 160−300 °C, the peak gradually shifted to higher values from 135 °C to 175 °C, suggesting that the improved metal-support interaction promoted with the increase in reduction temperature (< 300 °C). Interestingly, when the Ru/MgAl catalysts were reduced at high temperatures, namely >400 °C, the peak I shifted back to 120 °C with a shoulder peak was observed at 132 °C, suggesting the reduced metal-LDO support interaction compared with that of metal-LDH. It was observed that the strong interaction between Ru species and support favours the catalysis [98]. Ateeq *et al.* [100] reported that the TPR for nickel containing hydrotalcite was characterized for Mg-Ni samples of varying ratios, showed two peaks of H_2 consumption. The first peak observed was at 570 K corresponds to the discharge of NO_3 anions as NO_2 and the subsequent reduction of NO and N_2O. The second peak was observed at 705, 920 and 1000 K for respective samples for the reduction of NiO particles. When Mg content is increased the reduction of the nickel oxide decreases it can be compared with the decrease of the NiO crystal size. This behaviour is ascribed due to the formation of Ni aluminate band of nickel spinel type and decreasing the size the crystallite and hence it hinders their reducibility [100].

Methanation of i) CO and ii) CO_2

i) $CO + 3H_2 \rightleftharpoons CH_4 + H_2O,\ \Delta H^o\ 298 = -206\ kJ/mol$ (1)

ii) $CO_2 + 4H_2 \rightleftharpoons CH_4 + 2H_2O,\ \Delta H^o\ 298 = -165\ kJ/mol$ (2)

Figure 2. CO_2, CO methanation reactions [99].

5. Applications of LDH Catalysts

5.1 CO_2 Methanation

Among the catalytic reactions, the reduction of CO and CO_2 with transition metal catalysts to form methane, (methanation reaction) is a favourable method for the removal of carbon oxides resulted in the manufacturing of various energy carrier products [101]. Few decades ago, methanation reactions have received substantial attention as an effective method to produce natural gas substitute, where coal is oxidized to CO and H_2 followed by accumulation to the formation of methane. Generally, methanation

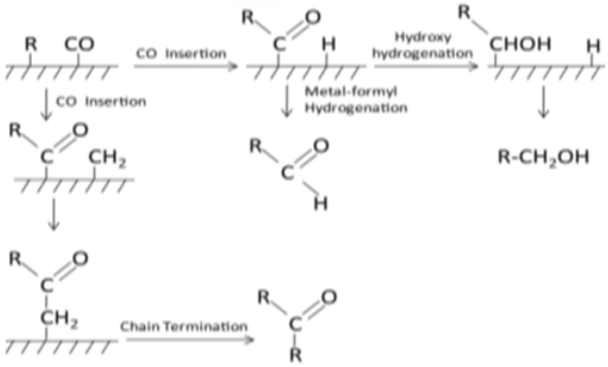

Figure 3. C_2 oxygenates by Fischer-Tropsch synthesis of carbene [101].

reaction is applied in ammonia plants at the final stages of purification for the synthesis gas insitu with the formation of low concentrations of CO and CO_2 at 0.1–0.5% are catalytically removed in the presence of hydrogen (Figure 2). The reaction is very important due to the poisonous or synergistic outcome of carbon oxides for ammonia synthesis reported by Xavier *et al.* [102]. Further, Xavier *et al.* [102] reported that the CO_2 methanation reaction with M^{2+} and M^{3+} cations, with their proportion, with wide range of LDH compositions are obtained, which addresses methanation reaction as potential process to produce fine chemicals.

Santos *et al.* [103] reported synthesis of Co-Al LDHs nano sheets produces selective oxygenates, of C_2 oxygenates, for Fischer-Tropsch synthesis of carbene insertion (Figure 3). Figure 3 represents the Fischer-Tropsch synthesis of carbene for the formation of oxygenates [103].

5.2 Cyanoethylation Reaction

Octavian *et al.* [104] reported cyanoethylation with LDHs MMgAlO catalysts (M = Mn, Fe, Co, Ni, Cu or Zn). The results of the catalytic cyanoethylation reaction of methanol with LDH catalysts exhibited high selectivity of 99–100% in β-metoxypropionitrile (CH_3–O–CH_2–CH_2–CN), while the conversions were very low. The latter remained in all cases lower than 5% after 5 h of reaction and ranked as follows: MgAl-LDH > CoMgAlLDH ≈ CuMgAl-LDH ≈ MnMgAl-LDH > FeMgAl-LDH ≈ ZnMgAl.LDH > NiMgAl-LDH. The cyanoethylation reaction with MgAl LDH conversions were lower i.e ~20% at 5 h with ethanol. This is attributed due to the proton abstraction which is easier on methanol with higher acidic character than ethanol which was not the rate limiting step [104]. However, with the lower conversions values observed for MMgAl-LDHs compared to the MgAl-LDH sample must be related to the lower intrinsic basic character of the former samples which decreased their ability to abstract a proton from the hydroxyl group of methanol. That was ascribed due to the higher electronegativity of the transition metal cations than Mg^{2+} which decreased the electron density on the hydroxyl groups of the MMgAl-LDH layers. Assuming that the latter are the catalytic sites, due to which their activity decreased.

5.3 Cyanosilylation of Aldehydes

Fahimeh *et al.* [105] reported that the cyanosilylation of aromatic aldehydes with MgAl-Cu LDHs catalysts (Figure 4). These catalysts have been tested in different organic transformations in recent years reported by Choudhary *et al.* [71]. Fahimeh *et al.* [105] reported the catalytic activity in different parameters such as percentage of catalysts employed, catalyst loading and effect of solvent for cyanosilylation at room temperature were evaluated. 20 mol% of LDHs catalyst were effective for cyanosilylation in dichloromethane solvent with quantitative yield in 30 minutes duration of time (Figure 4).

5.4 Oxidation of Alcohols with Ni-Al

Rahman *et al.* [106] reported for the first time reported a shortest route for molecular oxygen activation by Ni-Al hydrotalcite for selective oxidation of various substituted α-ketols, benzylic and allylic alcohols to carbonyl compounds. They studied the comparison of Cat A, Cat B and Cat C with Ni-Al ratios of 2:1, 2.5:1 and 3:1 and found that the best results with Ni-Al 2:1 ratio. Cat B with Ni-Al ratio of 2.5:1 was synthesized by co-precipitation method with ammonia as base. All these catalysts were subjected to longer duration of time for the reaction compared to Cat A with 2:1 Ni-Al ratio which took 6 h for the completion of reaction. Other ratios 2.5:1 and 3:1 Ni-Al took 10 to 20 h for the completion of reaction. This is ascribed due to the formation of more Ni ions during the preparation of catalysts. One of the notable achievements of this methodology was Cinnamyl alcohol was oxidized to Cinnamaldehyde without disturbing the double bond [106].

5.5 Reduction of Aldehydes to Alcohols with Ni-Al

Choudhary *et al.* [71] have reported with different ratios of Ni-Al hydrotalcites were used in the reduction of aromatic, heterocyclic aldehydes to alcohols. Different moieties of aro-

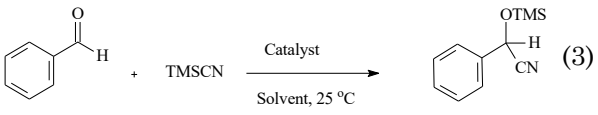

(3)

Figure 4. MgAlCu LDHs is used for cyanosilylation of carbonyl compounds [91].

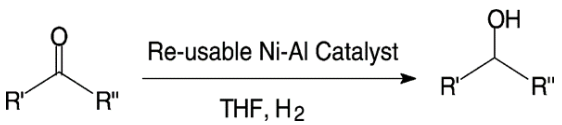

(4)

Figure 5. Ni-Al hydrotalcite calcined catalyst for reduction of aldehydes to alcohols [71].

matic and conjugated aldehydes, and heterocyclic aldehydes were subjected for the reduction of aldehydes to alcohols selectively in the presence of other susceptible functional groups. Figure 5 equation (4) shows the reported Cinnamaldehyde that was reduced to Cinnamyl alcohol without affecting the double bond. Hence, it is well known that Ni catalyst reduces the double bond in aliphatic and aromatic compounds.

Rahman *et al.* [107] reported the reduction of aromatics to alicyclic molecules with super active 2:1 Ni-Al hydrotalcite catalysts to alicyclic without loss of activity of the catalysts. Osmate intercalated hydrotalcite aimed at selective oxidative bromination of bisphenol-A for asymmetric dihydroxylation of olefins [108] with NMO (N-Methylmorpholine N-oxide) used as co-oxidant in company of molecular oxygen was reported by Choudhary *et al.* [108].

5.6 Reductive Amination of Benzaldehyde with Ni-Al LDHs

Rahman *et al.* [106] reported the reductive amination of benzaldehyde with ratios of 2:1, 2.5 and 3:1 Ni-hydrotalcite catalysts which exhibited good catalytic activity for synthesis of amines. Ni-hydrotalcite catalysts for reductive amination of benzaldehyde with $NaBH_4$, acts as reducing agent to form in situ-Ni-boride which is generated swiftly in the formation of desired product at room temperature. The activity of Ni-Al hydrotalcites for organic transformation discussed above is attributed due to the even distribution of Ni ions for 2:1 ratio of Ni-Al hydrotalcite catalysts and inactivity of 2.5:1, and 3:1 ratio catalyst is due to higher content of Ni in Ni-Al hydrotalcite [107].

5.7 NO_x Reduction

Cu/Co/M (where M = Al, Fe, Cr, Ni and Fe) mixed oxides and Mn-LDHs have been studied for NOx reduction to evaluate the catalytic activity of mixed metal oxides. Polmeres *et al.* [109] reported selective reduction with mixed oxides at high temperatures resulting from LDHs. Numerous methods have been used for the reduction of NO_x emission. Primarily the conventional procedures for NO_x reduction with NH_3 (ammonia-SCR) [109]. SCR of NO_x is an extremely efficient method to reduce NO_x emissions in oxygen-rich exhausts. In the area of NO_x reduction, mixed metal oxides based catalysts have been extensively studied due to high hydrothermal stability of LDHs catalysts [109]. Nonetheless, the ammonia-SCR is non-environment friendly process. Hydrocarbon acts as excellent reductant for NO_x (HC-SCR) that entices more interests due to its short price [109]. The emergence of LDHs, catalysts generated potential interests as catalysts for removal of NO_x from diesel exhaust gases [109]. LDHs have exhibited excellent catalytic activities on SCR of NO_x in the presence of SO_2 and H_2O at low temperature. Palomares *et al.* [109] have reported that the behavior of soot combustion with NO_x/O_2 with potassium-supported Mg-Al hydrotalcite with in situ FT-IR spectroscopic studies confirmed the presence of NOx in O_2 favors the combustion of soot at lower temperatures (<573 K) [110]. Adamski *et al.* [110] reported that the $nFeO_x@TiO_2$ catalysts possessing the core-shell structure demonstrates that the excellent catalytic activity on SCR of NO_x with NH_3 which acts as reductant [110].

5.8 Polymerization of Propylene Oxide with LDHs Catalysts

Olena *et al.* [111] reported for the first time that LDHs as heterogeneous catalysts for polymerization of propylene oxide. Does not require complex post-reaction separation of the catalyst. Laycock *et al.* [112] reported polymerization of Propylene oxide with thermally activated synthetic MgAl LDHs. Meanwhile, in similar conditions, yields an optically active crystalline fraction and a liquid fraction of considerably reduced optical activity. Both liquid fractions exhibit a high degree of region-irregularity in the polymer chain [112].

5.9 Ring Opening Reaction of Styrene Oxide with LDHs Catalysts

Kantam *et al.* [72] reported the ring opening of styrene oxide with nucleophiles $TMeSiN_3$, TMeSiCN, and $MgAlCO_3$ hydrotalcite catalysts which resulted in ring opening products with high conversion and selectivity. $MgAlCO_3$ hydrotalcites displayed reusability up to 3 cycles with high reproducibility, which exhibits the good catalytic activity of $MgAlCO_3$ hydrotalcite for ring opening of epoxides.

Tengfei Li *et al.* [113] reported the catalytic activity of Zn_3Al-CoW_{12} for aminolysis of epoxides. They further reported that the aminolysis of styrene oxide with aniline did not proceed in the absence of a catalyst while a small amount of aminolysis product ($< 8\%$) is obtained in the presence of Zn_3/Mg_3Al-NO_3 as a catalyst. The $K_5CoW_{12}O_{40}$ cluster demonstrated the higher catalytic activity, in comparison to $Na_3PW_{12}O_{40}$ and $K_4SiW_{12}O_{40}$ with similar structure. These results reveal the superior performance of the

CoW_{12} anions for the catalytic aminolysis of epoxides with aniline and subsequent formation of ß-amino alcohol-based products. Particularly, the utilization of the Zn_3AlCoW_{12} as heterogeneous catalyst, demonstrated good catalytic activity although seems that the diffusion and mass transfer have an influence on the activity of the heterogeneous reaction to some extent. This may be ascribed due to the regular porous structure of the intercalation material which induces enhanced accessibility and shorter diffusion pathways during the course of the catalytic reaction [113].

5.10 Ester Epoxidation with LDHs Catalysts

Ester epoxidation has been reported in literature with solid catalysts intercalated with metalloporphyrins, methyl rhenium trioxide, zeolites and aluminium-based catalysts [114–115] were active catalysts for epoxidation of FAMEs. Li *et al.* [116] reported the use of phosphotungstic acid (HPW)/Mg-Al LDHs, Zn-TiO_2 LDHs as active catalysts for epoxidation of FAMEs in Table 2 [116].

5.11 Suzuki Coupling Reaction with LDHs Catalysts

Several LDHs modified photo catalysts have been developed in the past for various reactions [117,118]. On contrary, a novel active LDHs photo catalysts which meets the current technical requirements by doping/deposition of various noble metals on LDHs. From the above considerations LDHs photocatalysts meets the criteria for the better investigation in the area of solar energy. AuPd alloy loaded on ZnCr-LDHs have been prepared for reduction reaction. ZnCr-LDHs has emerged as superior catalysts and has developed as a super active catalyst for Suzuki coupling reaction [118]. Parida *et al.* [117,118] reported that the synthesis of LDH@AuPd and LDH@Pd: Zn-Cr LDHs by co-precipitation method with a molar ratio of 3:1 at pH 11. Sahoo *et al.* [119] however, reported the synthesis of APTES functionalized LDHs.

Parida *et al.* [117,118] reported that the photo catalytic reaction of Suzuki coupling with LDH@AuPd catalyst. The biphenyl yield increases frequently with the effect of time after 2 h of irradiation. Hence, biphenyl product

Table 2. Epoxidation of FAMES with H_2O_2 conversion and selectivity [116].

No	Catalyst	Conversion (%)	Selectivity (%)
1	HPW-Zn-Ti LDH	85.4	82.2
2	HPW-Zn-Ti-3 LDH	90.6	86
3	HPW-Zn-Ti-4 LDH	87.1	79.5
4	HPW-Zn-Al-3 LDH	63.4	20.2
5	Zn-Ti-2 LDH	52.2	8.1
6	Zn-Ti-3 LDH	55.1	9.2
7	Zn-Ti-4 LDH	56.3	8.4
8	$Zn(OH)_2$	4.8	16.5
9	$Ti(OH)_2$	2.9	23.4
10	$Na_3[PW_{12}O_{40}]$	17.8	8.2

* Reaction temperature - 70 °C ; reaction time - 7 h; $n(H_2O_2)/n$ (double bond), 1.5:1; m-catalyst/m (reactants), 0.07:1.

Table 3. A comparison of heterogeneous Pd based catalysts reported in the previous reports with our study towards Suzuki cross-coupling reactions [117-119].

Entry	Catalysts	Conditions (h, °C)	Conversion (%)
1	XLPd	115	86
2	0.01 mol% Pd-CD	24 h, 60	100
3	PdTNs	1 day, 20	100
4	Pd/MCM-41	5 h, 78	93
5	LDH-DS-Pd	5 h, 80	93
6	Silica-APTS-Pd	2 h, 100 °C	99
7	Pd@LDH in the present	10 h, 80 °C	96
8	AuPd bimetallic alloy NPs	2 h, Room temp,	98

is formed with a maximum of 98% yield. To optimize the quantity of catalysts, a series of LDH@AuPd photo catalysts were executed and was observed that the catalytic activity with 0.1 g was excellent (Table 3).

5.12 Esterification with LDHs Catalysts

2-Ethylhexanol is converted on acidic and basic sites of LDHs catalysts to desired products. For example, the oxidation of 2-ethylhexanol to 2-ethylhexanal [120] usually takes place on acid-base sites of catalysts [121] with a minimum content of Al [121]. Successively, 2-ethylhexanoic acid to 3-heptanone [121] is achieved via Ketonization on active sites of LDHs catalysts [122]. Moreover, 3-heptanol is formed by the reduction of 3-heptanone over basic sites of LDHs [121,122]. It could be observed that all the reactions are directed by the properties of acidic and basic sites of catalysts. Hence, mixed oxide catalysts that are derived from LDHs are more favorable catalysts for many reactions that is easily modified and tuned by changing their elemental compositions.

5.13 Electrodeposition Reaction with LDHs Catalysts

The electrodeposition process is frequently used to formulate a self-supported LDHs films on conductive substrates in a two- or three-electrode alignment. The substrate is active as working electrode, whereas an aqueous solution comprising of metal salts performs as an electrolyte in this method. Hence, the reduction reaction between the metal and OH^- ions leads to the creation of a self-supported LDHs nano catalysts on the substrate. This method is simple, and eco-friendly process which is completed within few minutes [123,124].

5.14 Oxygen Evolution Reaction (OER)

Recently research has been focused on supported LDHs for OERs [123,124]. Hence, hydrogen production by electrochemical water splitting is very effective and provides a greener method compared with traditional process of steam-reforming method which produces hydrogen from the natural gas [125,126]. Generally, the OER reaction is divided into three successive stages: adsorption of water molecules on surface of catalyst, water splitting reaction into molecular oxygen by intricate process, and finally the release of molecular oxygen [127]. Subsequently, LDHs material can dissolve in acidic conditions, they are carried out in KOH solution. The general reaction of OER process in alkaline media are shown in Scheme 1 [128].

$$OH^- + * \longrightarrow OH^* + e^- \quad (5)$$

$$OH^* + OH^- \longrightarrow O^* + H_2O + e^- \quad (6)$$

$$OH^- + O^* \longrightarrow OOH^* + e^- \quad (7)$$

$$OOH^* + OH^- \longrightarrow O_2 + * + H_2O + e^- \quad (8)$$

Scheme 1. Reaction of OER process in alkaline media [123,124].

Scheme 1 signifies the adsorption site on the electro catalyst and O^* and OH^* denotes as adsorbed intermediates. Each step presented above in Scheme 1 creates one electron, hence, the OER process works in alkaline media by four-electron transfer. The catalytic progress of specific OER method is initially assessed by cyclic voltammetry (CV) and linear sweep voltammetry (LSV) testing method. Though, to judge the OER performance of a particular catalyst, very crucial parameters include over potential (η), Tafel plot (b), exchange current density (j_0), and turnover frequency (TOF), are vital for this reaction [128,129]. Furthermore, OER plays a vital role in energy-conversion systems such as CO_2 reduction, fuel cells, and metal–air batteries and energy-storage [130,131]. The electro catalyst, that reduces the overall potential which is essential for water splitting as a result of lowering the activation energy, which is broadly engaged to maintain the OER kinetics [131]. The conventional precious-metal-based electro catalysts such as IrO_2 and RuO_2 displays excellent OER reaction [131]. Rahman and co-workers [132] recently reported OER reaction review with Ni LDHs nano platelets. Recently there have been many articles reported on water splitting which facilitates the production of hydrogen by direct route for water splitting into hydrogen and oxygen [132]. Though, the energy necessary to cleave H and O−H bonds is provided by diverse power sources such as i) Electrical (current), ii) Thermal (heat), or iii) Light (electromagnetic radiation). Despite the enormous industrial applications of hydrogen, there are further possibilities for research expanding in area of water splitting with use of LDH catalysts. Among the various renewable energy technologies for hydrogen production from water splitting, photocatalytic and photo electro-chemical (PEC) methodologies has been broadly reflected as energy technologies devoid of environmental pollution [132,133].

5.15 Nickel Based Layered Double Hydroxides for Water Splitting

Rahman and co-workers [132] reported various NiFe-based catalysts for water splitting reaction and developed the active phase and provided a detailed mechanism of NiFe based compounds. However, there is no article till date on categorizing the structure and the pathway, both theoretically and experimentally, during OER electro catalysis [133,134]. The earliest interrelated mechanistic studies reported that the active phase of $Ni(OH)_2$ or nickel oxide (NiO_x) catalyzing OER. Hence, the phase transformations of $Ni(OH)_2$-based electrode tracks the Bode's diagram with β-$Ni(OH)_2$ and α-Ni(OH)2 altering into β-nickel oxyhydroxide (β-NiOOH) and γ-NiOOH correspondingly during charging and discharging γ-NiOOH which is derived from overcharging β-NiOOH, whereas α-$Ni(OH)_2$ converts into β-$Ni(OH)_2$ [134]. Various studies on the influence of Fe deposition on Ni-based OER electro-catalysts was additionally evaluated by few methods, such as density functional theory (DFT) calculation and in situ spectroscopy [132–134].

5.16 Advantages of LDHs for OER Reaction

LDHs materials, principally Cobalt, and Nickel containing LDHs, are the most favourable materials, that shows innovative method for OER electro-catalytic performance outperforming additional non-precious metal based OER electro-catalysts. LDHs have numerous advantages in contrast to 0D and 1D materials such as bulk surface-to-bulk ratios, surface area, particle size distribution, morphology and efficient exposure of catalytic active sites. These properties derive the catalysts as excellent LDH materials for OER reactions [134].

6. Other Applications of LDHs

6.1 LDHs Catalysts as Filler in Concrete

The carbon foot mark of concrete production industry is rapidly emerging as larger economy in South-Asian regions that are concentrating on swiftly development of infrastructure. Additionally, the conventional methods have contributed to environmental related issues for cement production [135,136]. Hence, to decrease the environmental impact of cement production, it is necessary to develop concrete infrastructure to reduce environmental related issues with longer shelf life. LDHs are used as cement additive that emerged towards the end of the 20th century. Nevertheless, with various degradation phenomena related with the reinforced concrete models, such as steel corrosion [137,138], freeze thaw cycles [139], ice abrasion [140,141] and acid attack [142]. The LDH finally formed was applied as a chloride entrapping additive with 8.5 wt% dosage in cement pastes and there were enhanced chloride uptake capabilities. Hence, Yoon *et al.* [143] reported the positive impact of LDHs in increasing the service life of concrete structures. Yoon *et al.* [143] have reported the use of commercially available Mg-Al LDH and calcined at 450 °C. It has been well documented that the interlayer anions in LDHs galleries could be exchanged easily with an anion molecule.

Owing to the above stated ion exchange property [144], this exclusive property portrays LDHs as a flexible material however, they can sequestration anions from the environment

Table 4. Effect of addition of LDH on the mechanical properties of concrete for compressive strength (CS) [145].

LDHs	Cement	Dosage	Concrete Properties		Age	Year
			CS	FS		
Ca-Al LDHs	Cem 42.5	1–5%	+6% (2%LDH)	-	28d	2009
MgAl CO_3		1–2%	inconclusive	-	28, 48d	2013
MgAl LDH	8.5%		~–2%	-	28d	2014
MgAl pAB	Cem I 42.5N	5–10%	–17.2% (10%LDH)	–21.38% (10%LDH)	28d	2015
MgAl NO_2	Cem I 42.5N	5–10%	–14.2%	–19.1% (10%LDH)	28d	2015
MgAl LDH		1%	–25% (28d)	-	8-178d	2015
LiAl LDH		1–3%	+25%	-	7d	2017
CaAl NO_3	Cem I 52.5R	0.5–2 Vol.	+17% (1% LDH)	+55%	28d	2018
MgAl CO_3	Cem I 52.5	1–3%	~+3.5% (3% LDH)	-	28d	2018
MgAl LDH		1–2%	+8.2% (1% LDH)	-	56d	2018
LiAl LDH		0.5–1.5%	+46.2% (1%LDH)	-	28d	2019

*CS = compressive strength, FS = Flexural strength

with an option of discharging a tailored anion. LDHs are consequently used as potential additive for the imprisonment of corrosion causing types of materials and discharging of corrosion preventing anions in cementitious environments. In concrete research technology, LDHs are nanoparticles which have been reported to polish the microstructure of concrete without increase in porosity [145]. Although, LDHs is regularly added in its powdered form to be distributed in the matrix. However, these LDHs nanoparticles are homogenously distributed during cement hydration process. Hence, LDHs can deliver extra nucleation sites during cement hydration. This further promotes growth of CSHs gels into the cavities, thus refining the microstructure. Furthermore, these particles perform as micro-fillers inside the cementitious matrix. It is provisional on the type of LDHs used, which will require a positive effect on the mechanical properties, such as compressive strength (CS) of concrete (Table 4). The LDHs usually have hexagonal platelet structures. Although they are capable of retaining their structure in concrete, the resulting concrete exhibits a superior flexural strength (FS) as LDHs possess thin platelets that acts as micro-beam elements flanked by cementitious materials and as a result it helps in effective transfer of bending stresses [145]. Table 4 presents a comprehensive data on flexural strength enhancement of concrete with different types of LDHs and doses used by different authors.

6.2 LDHs as Filler for Polymer

There are many literature reports pertaining to montmorillonites and cationic clays, suggested on the application of organic modified hydrotalcites are efficient fillers of polymers, for example polyethylene, polystyrene and polymethylmetacrylate [146] which gave excellent results for mechanical strength [146]. Jiao [146] reported that the MgAl-CO_3 showed as an efficient halogen-free flame retardant additive, which performs as Heat Release Rate (HRR) reducer and as a remarkable smoke suppressant [147]. It has been reported that the MgAl-CO_3 has a better flame retardant efficacy than either MH (Magnesium hydroxide) or AH (Aluminium hydroxide) as flame retardation of EVA [147,148]. Costache *et al.* [149] reported that the phosphorus compounds act as efficient halogen free flame retardants and are often used alone or in combination with MH or AH, that increases the conversion of organic matter to charred sheets during combustion. Hence, these charred sheets will lower the amount of flammable volatile gases that reaches the flame zone and reduces the heat transfers from the flame to the polymer.

Prasad *et al.* [150] reported that magnetic Fe_3O_4 based LDHs nanocomposites (Fe_3O_4/LDHs) on the synthesis, properties and applications. Generally, the properties of optimal magnetic Fe_3O_4/LDHs photocatalytic assembly aim to come across the following requirements. (i) The preparation and manufacturing process of (Fe_3O_4/LDHs) are very simple with good yield. (ii) Magnetic Fe_3O_4-LDHs composites exhibits greater photocatalytic performance of Fe_3O_4 and pure LDHs sample. (iii) Magnetic Fe_3O_4/LDHs photo catalysts should be reprocessed through exterior magnetic field which can be easily regenerated and recycled. Finally, the Fe_3O_4/LDHs photo catalyst possesses an outstanding photo corrosion resistance capacity and should be very stable at room temperature. Daud *et al.* [151] have reported that the graphene/LDHs nanocomposites have emerged as new advances in the area of material science. Here, the methods utilized for the synthesis of magnetic Fe_3O_4/LDHs nanocomposites and their key applications in the classical area of photo catalysis and environmental remediation were studied [151].

6.3 LDHs Acts as Host for Drugs

The author's in this section present drugs as excellent materials to intercalate in LDHs due to negative charges species. Nalawade *et al.* [152] reported that the LDHs are excellent hosts for negatively charged species which provides better methods of drugs and genetic materials that are introduced into cells. Consequently, if it is consumed, biomolecules-LDH nano-hybrid can transfer across the mucous membrane of the intestine. However, neutral hybrid may enter the cells by moving diagonally, where negative charged cell membranes without being repulsive electrostatic interactions that could be experienced alone by guest anion species. When inside the cell, the LDHs are broken down by lysosomes the resulting intercalate anion is released [152].

Biomolecules are stable in LDHs lattice. If required, de-intercalated by ion-exchange method with atmospheric CO_2 or other anions. These exceptional characteristics will permit LDHs to be utilized as new drug or gene carriers if transmission is effective of bio hybrids to cells are proved. Hence, to evaluate the transfer efficiency, isotope-labeled [^{32}P] ATP–LDHs hybrid was synthesized by ion exchange method and application of such hybrids by eukaryot-

ic cells was examined for incubation time taken. Exogenously introduced ATP–LDHs hybrid enters into HL-60 cells efficiently in shorter duration of time. However, transfer effectiveness was found to be greater up to 25-fold in 2 h duration of incubation, for ATP only. However, after 4 h of incubation, the uptake level of hybrids becomes lesser to 12-fold. In comparison, the hybridization between ATP and LDHs it neutralizes surface charge of anionic phosphate groups in ATP, which is attributed to the cationic charge of LDHs, which results into favorable endocytosis of cells, and finally results into better transmission efficiency [152,153].

Adding LDHs to a solution of desired drugs in water at room temperature results in intercalation of these molecules in LDHs. LDHs swells up to 20 Å and can occupy the size of guest molecules. LDHs have excellent property of possessing antacid and antipepsin properties. Branded antacids products (TALCIDTM and ALTACITETM) contain LDH $Mg_6Al_2(OH)_{16}CO_3$. Drugs such as Diclofenac (DIC), Ibuprofen, Naproxen, Gemfibrozil, 2-Propylpentonoic acids, 4-Biphenylacetic acid, Tolfenamic acid, indomethacin, ketoprofen, tiaprofenic acid and flurbiprofen can be intercalated into LDHs [154]. Numerous cardiovascular, anti-inflammatory agents such as carboxylic acids or carboxylic acid derivatives, can be intercalated in LDHs by ion exchange method. However, intercalating into LDHs modifies Diclofenac (DIC) discharge, the interlayer region of this matrix is considered as micro vessel, in which the drug is stored and released by de-intercalation method due to the ions present in small intestine [154]. The release of Diclofenac (DIC) usually depends on diffusion through particle size and not on concentration of drug. In vitro studies it shows that the drug is free by a de-intercalation procedure due to interchange of drug with ions present in dissolution medium [154]. Hence, it is observed that the drug is released from LDHs at pH 7.5. Hence, the drug is discharged from LDHs DIC is much slower than that from mixing, which is completed in 9 hours. Kinetic analysis results have observed that there is diffusion through particle in controlling drug discharged. Therefore, it is very important that the reversible intercalation of wide variety of active cardiovascular and anti-inflammatory agents into LDHs that can result into new tunable drug delivery system [153]. Umberto *et al.* [154] (Table 5) reported that in order to examine the catalytic aptitude of MgAl hydrotalcites to intercalate the L-DOPA (L-3,4-dihydroxyphenylalanine) that is structurally identical to amino acids which are used as drug in the Parkinson's disease. Umberto *et al*. [154] reported that at pH 9 intercalation is accomplished, with hydrazine as an antioxidant. Table 4 reports the interlayer distance of intercalated compounds with amino acids bearing two carboxylic groups as glutamic (Glu) and aspartic acid (Asp) and composition of LDHs.

6.4 LDHs as Guest Species for Antimicrobial and Antioxidant Activity

However, the intercalation of the biologically active class into hydrotalcites that exhibits antimicrobial activity for benzoate (Bz), 2,4-dichlorobenzoate (BzDC) and para- and ortho-hydroxybenzoate (p-BzOH, o-BzOH) [154]. The composition of the materials is presented in Table 5 [155] directs that the benzoate, and benzoate derivatives of anions easily replaces the nitrate counter-anions finally, whereas the Fer and the Asc exchange for 53% and 31% to nitrate or chloride anions.

6.5 LDHs Composite Materials

Usually, Fe Magnetic LDHs are prepared by co-precipitation, hydrothermal, and solvothermal methods [156,157]. The hybrid materials of LDHs nanocomposite and Fe_3O_4 MNPs is highly recommended for environmental pollution control. There are few published articles studied on the synthesis of Fe_3O_4/LDHs nanocomposites and for their photocatalytic applications [157] (see Table 6). The magnetic separation of Fe_3O_4/LDHs materials have been exam-

Table 5. Composition and basal spacing (*d*) of the indicated intercalation compounds dried at 75% of relative humidity [155].

	Acronyms	Composition	*d* (Å)
Antimicrobial	Zn-Al-Bz	[ZnAl]0.35Bz0.35. $1H_2O$	15.5
	Zn-Al-O-BzOH	[ZnAl]0.35o- BzOH0.27(NO_3)0.08.1 H_2O	15.5
	Zn-Al-P-BzOH	[ZnAl]0.32 p-BzOH0.33(NO_3)0.02.1 H_2O	15.3
	Zn-Al-BzDC	[ZnAl]0.32 BzOH0.32(NO_3)0.03.1 H_2O	16.8
Anti-oxidant	Mg-Al-Fer	[MgAl]0.36(Fer)0.19(NO3)0.17.0.89 H_2O	17.3
	Mg-Al-Asc	[MgAl]0.36(Asc)0.11Cl0.25.0.29H_2O	12.8

Table 6. Synthesis and applications of magnetic Fe_3O_4/LDHs nanocomposites [165].

Nanocomposite	Method of preparation	Size (nm)	Application	Reference
Fe_3O_4Mg Al-LDH	Coprecipitation Synthesis	40–100	Adsorption properties of dye from water	[158]
Mg-Al-Fe-CO_3-LDHs	Coprecipitation Synthesis	–	Photocatalytic activity of H2 generation	[159]
Fe_3O_4-MgAl-LDHs	Coprecipitation Synthesis	–	Adsorption of Cd(II)	[160]
Core shell Fe_3O_4-CuMgAl-LDHS	Co-precipitation Synthesis	100–200	Hydroxylation of phenol	[161]
Core shell Fe_3O_4-CuMgAl-CO_3LDHS	Co-precipitation	300–350	Anionic dye removal from wastewater Hydroxylation of phenol	[161]
LDHs-Fe_3O_4 magnetic nano hybrids	Mixed method (co-precipitation synthesis and hydrothermal method)	240	Thermo-chemotherapy	[162]
Mg-Al LDHs-Fe_3O_4 nano composites	Two-step wet Chemistry route	10–20	Removal of humic acid	[163]
Fe_3O_4/(Cu/Ni)–Al LDHs	Co-precipitation synthesis	10	Degradation of methylene blue	[156]
Fe_3O_4/sulfonated LDHs β-cyclodextrin intercalated	Co-precipitation method	200	Methylene blue removal	[164]
Fe_3O_4@C@Ni–Al LDHs	Two-step layer- by-layer route	10	Separation of uranium	[165]
Fe_3O_4/ZnCrLDHs	Two-step microwave treatment hydrothermal method	10	Organic dyes wastewater	[166]
Fe^{3+}doped Mg/Al/ LDHs	Solvothermal method	35–70	UV lights hielding coatings	[167]
Fe_3O_4/ZnAl–LDHs	Co-precipitation method	–	Removal of Cr(VI)	[168]
Fe_3O_4@DFUR–LDH	Co-precipitation	10–20	Magnetically controlled drug delivery	[169]
NiAl-LDH/Fe_3O_4-RGO Nanocomposites	Hydrothermal route	15	Degrade ciprofloxacin (CIP)	[170]
Fe_3O_4/Mg_2Al-NO_3- LDHs	Co-precipitation method	–	Remediation of aqueous phosphate	[170]
Fe_3O_4@MgAl–LDH@Ce_3W_{18} nano composite	Selective ion-exchange method	10–40	Degradation of methylene blue	[172]
Fe_3O_4@MgAl–LDH@Au	Solvothermal method	100–200	Catalytic oxidation of alcohols	[173]
Fe_3O_4/ZnCr LDHs	Two-step microwave hydrothermal method	20	Efficient removal of dyes and heavy metal wastewater	[174]
Fe_3O_4/MgAl-LDH composite	Co-precipitation method	–	Three red dyes (reactive red (RR), congo red (CR) and acid red)	[175]
Fe_3O_4@CuNiAl-LDH	Co-precipitation method	100	–	[176]
magnetite-graphene (MG) and Mg/Al LDHs	Hydrothermal process	1436.8	Adsorption of arsenate	[177]
Fe_3O_4/MTX-LDH/Au nanoparticles	Co-precipitation	255–270	For cancer therapy	[178]
Fe_3O_4/SiO_2/NiAl-LDH microspheres	Situ growth method	300	Magnetic separation of proteins	[179]
Fe_3O_4/GO/LDHs Composites	Mechano hydrothermal route	200	For removing the heavy metal Pb(II) and the hydrophobic organic pesticide 2,4-dichlorophenoxy-acetic acid.	[180]

ined in aqueous solution by placing the magnet near the glass, and it displays the magnetic properties of materials [157]. As a result, separating the magnetic Fe_3O_4/ZnCr LDHs nanohybrids swift variations are observed in the environmental remediation. Methylene blue (MB) is extensively utilized for photocatalytic studies as classical dye. The MB stability rises against photo catalysis when the pH is less, but the adjustment of pH to 5.4 will lead to suspension of hydrotalcite [157]. Further, Prasad *et al.* [150] reported that MB for 3 h at room temperature with Fe_3O_4/ZnCr LDHs nanocomposite removes ~95% of MB in aqueous solution. This result is much better when compared to ZnCr LDHs samples, hence degrades only 58.1% under UV-light in 3 h, this is due to Fe_3O_4/ZnCr LDHs nanocomposites confirms better catalytic activity, this is ascribed due to the increased surface area and its exceptional advantage being easy separation under external magnetic fields. These results are attributed due to the modification of Fe_3O_4 NPs on LDHs surface exhibits superior photocatalytic activity of ZnCr LDHs. Mardani *et al.* [156] reported that the Cu/Ni–Al LDHs/Fe_3O_4 nanocomposite were prepared by co-precipitation method. However, magnetic Fe_3O_4 (core) were prepared by co-precipitation for Fe^{2+} and Fe^{3+} in aqueous solution. Then further nanocomposite was synthesized by co-precipitation of Cu^{2+}, Ni^{2+}, and Al^{3+} metal ions on the Fe_3O_4 core nanoparticles in the alkaline medium. Prasad *et al.* [150] reported that the results of these analyses confirms that the magnetic nanocomposite of LDHs and Fe_3O_4 synthesized were stable in aqueous solution via electronic interaction forces.

6.6 Degradation of Dyes with LDHs

LDHs are widely utilized for catalytic reactions and as catalyst supports [181] and it is further used for treatment of printing and dyeing wastewater. LDHs have been well known as adsorbents and photocatalysts [182,183]. Due to the dual properties as surface adsorption and interlayer adsorption of anions, LDHs can effectively adsorb anionic contaminants in dyeing, printing, and wastewater [184-188].

6.7 Adsorption of Heavy Metals on LDHs

However, it is well known that the surface water pollution and groundwater contamination are environmental problems. The main sources of environmental pollution owing to heavy metal contaminants, such as copper, lead, cadmium, chromium, arsenic, and zinc, this is ascribed due to the mining industries which are toxic at lower concentrations posing environmental challenges. Based on the nature of mining, and the level of concentrations of metal ions are huge and varies. It is already known that heavy metal ions having high toxicity and reduced biodegradability for plants and animals at greater concentrations [189,190]. Kano *et al.* [191] reported that the adsorption of heavy metals on LDHs intercalated with chelating agents. Perez *et al.* [192] reported recently that the LDHs modified with chelating agents are crucial adsorbents of heavy metals. However, Perez *et al.* [192] reported that the ZnAl-NO_3, ZnAl-EDTA, MgAl-NO_3, MgAl-EDTA, and MgAl-EDDS are active catalysts for removal of contaminants from water. Kano *et al.* [191] reported the adsorption capacities of Cu(II) or Pb(II) onto L1, L2, L3, and L0. The adsorption effectiveness of Cu^{2+} was superior compared to Pb^{2+} for the similar absorbent, this is ascribed due to their stability constant (EDTA-Cu, EDDS-Cu, EDTA-Pb, EDDS-Pb. Gasser *et al.* [193–197] reported that due to the larger adsorption the capacity is obtained as the chelate-metal has high stability constant. Finally, it is concluded that the higher adsorption efficiency of L0 than L1 is attributed due to high specific surface area of LDHs [197–202] (see Table 1).

6.8 Intercalating of Chelating Agents on Metals with LDHs Catalysts

Kano *et al.* [191] reported that remarkable results were obtained for the LDHs intercalation with chelating agents on the adsorption of metals [198]. The adsorption of Cd(II), Cu(II), and Pb(II) onto these LDHs studied in optimal conditions were obtained as reported by Liang *et al.* [203]. LDHs were found to adsorb Cd(II), Cu(II), and Pb(II) from solutions, which increases with time during the uptake was observed. It was evident from the results that the adsorption capacity of both LDHs for Cd(II), Cu(II), and Pb(II) improved swiftly through all the stages, and subsequently increased regularly. However, the adsorption capacity of Cu(II) and Pb(II) was observed to be greater than that of Cd(II). It was reported that the heavy metals were adsorbed by LDHs consisting of two mechanisms: chemical precipitation and chelation [203]. In the initial case, the hydroxyl anions participate with chelating agents for the precipitation of metal hydroxides at a greater pH. In the second case, the adsorption affinity is usually evaluated by the stability constant of the analogous complex [165,166].

7. Future Outlook and Current Opinions on LDHs Catalysts

The key tenants on the future outlook and current opinion are highlighted as choice of metals, ions for development of reusable, reproducing of green catalysts by economic process. For the developed of value added products. Waste materials can have converted to LDHs catalysts, *i.e.* incorporating different metals to evaluate the potential use of waste materials into active LDHs green catalysts, that can be applied in different areas, such as environmental, engineering, medicine, renewable energy, and catalysis. A tunable catalyst with active metal center or sites, to be focused on for development of green process on the concept of green chemistry / green catalysts. Further future recommendations can be evaluated for fine tuning of LDHs under different parameters.

The key general areas investigated in the literature can be categorized as: The variables important to catalyst synthesis, characterization, and applications for different reactions. The commercial utilization of LDHs is very essential for the advancement of LDHs catalysts and requires a scalable continuous production technique to get high yield and high crystallinity. Hence, an integrated method could be employing microfluidic technology and tubular reactors needs to be explored in detail, towards the sustainable mass-scale production. Although LDHs effective work's for various organic transformations, medicine, environmental, flame retardants and many of areas of science and engineering. However, for the effective industrial applications, it is highly recommended to assess the performance of these LDHs at industrial level in order to replace the conventional catalysts.

8. Concluding Remarks

The aim of this review is to study new techniques developed for the preparation, characterization and applications of LDHs catalysts. LDHs acts as green catalysts that can be applied in the absence of conventional catalysts used. Green chemistry focusses on the environmental aspects of both chemical products and the technology by which they are produced. LDHs catalysts are green catalysts that eliminates wastes and avoids the use of toxic and or hazardous reagents and solvents in the manufacture of fine chemicals. The surface area of LDH is measure by N_2 Physisorption which varies between 230 cm^2/g and 102 m^2/g depending, mainly on the active sites of LDHs catalysts. A typically crystalline structure of LDH is Rhombohedral and this can be verified by XRD analysis. SEM evaluates the surface morphology of LDH. Through XPS one can determine the chemical and pattern of the electronic structure of the surface of LDH. The surface area of LDH and adsorption-desorption process can be characterized by BET surface area. FT-IR spectroscopy is vital to determine the functional group such as OH, Carbonate, and polymer intercalated in LDH. The vibration, rotational and molecular aspects are evaluated by Raman Spectroscopy. The DTA-TGA method is applied for Measuring the variations in Mass at different temperature. The surface chemistry of metals and metal oxides are characterized by Temperature Programmed Reduction (TPR) under various thermal conditions in order to evaluate the application of reducing gas mixture that are adsorbed on the metal or metal oxide surface. However, modified LDHs catalysts can be developed for studying new applications due its tunable nature of LDHs, and excellent properties it exhibits due its active sites, memory effect, reusability, stability for longer reactions, regardless of reactions parameters applied, simple method of synthesis, economic and eco-friendly process can be developed. However, the authors evaluated that the most important and recent achievements have been reviewed on LDHs catalysts, and future recommendations have been evaluated with the ultimate goal to offer a panoramic vision of the importance and potential of this branch of material science.

Funding

Rajasekhar Pullabhotla would like to acknowledge the National Research Foundation (NRF, South Arica) for the financial support in the form of the Incentive Fund Grant (Grant No: 103691) and Research Developmental Grant for Rated Researchers (112145).

Acknowledgments

The author's acknowledge's University of Zululand, South Africa and University of Namibia, Windhoek, Namibia. To support this project. Rajasekhar Pullabhotla would like to acknowledge the National Research Foundation (NRF, South Arica) for the financial support in the form of the Incentive Fund Grant (Grant No: 103691) and Research Developmental Grant for Rated Researchers (112145). Finally, authors would like to acknowledge Mrs. Rakshana Pullabhotla for the editorial service.

References

[1] Paulo, L., Benıcio, F., Silva, R.A., Lopes, J.A., Eulalio, D., dos Santos, R.M.M., de Aquino, L.A., Vergutz, L., Novais, R.F., da Costa, L.M., Frederico G. P., Jairo. T. (2015). Layered Double Hydroxides: Nanomaterials for Applications in Agriculture. *Rev. Bras. Ciênc. Solo*, 39, 1–13, DOI: 10.1590/01000683rbcs20150817.

[2] Taylor, H.F.W. (1973). Crystal Structures of Some Double Hydroxide Minerals. *Mineral. Mag.*, 39, 377–389. DOI: 10.1180/minmag.1973.039.304.01 .

[3] Ren, L., He, J., Evans, D.G., Duan, X., Ma, R. (2001). Some Factors Affecting the Immobilization of Penicillin G Acylase on Calcined Layered Double Hydroxides. *J. Mol. Catal. B: Enzymatic*, 16, 65–71. DOI: 10.1016/S1381-1177(01)00044-3.

[4] Albertazzi, S., Busca, G., Finocchio, E., Glckler, R., Vaccari, A. (2004). New Pd/Pt on Mg/Al Basic Mixed Oxides for the Hydrogenation and Hydrogenolysis of Naphthalene. *J. Catal.*, 223, 372–381. DOI: 10.1016/j.jcat.2004.01.024.

[5] Fan, G., Li, F., David, G.E, Xue, D. (2014). Catalytic applications of layered double hydroxides: recent advances and perspectives. *Chem. Soc. Rev.*, 43, 7040-7066. DOI: 10.1039/C4CS00160E.

[6] Kirm, I., Medina, F., Rodrıguez, X., Cesteros, Y., Salagre, P., Sueiras, J. (2004). Epoxidation of Styrene with Hydrogen Peroxide Using Hydrotalcites as Heterogeneous Catalysts. *Appl. Catal. A*, 272, 175–185. DOI: 10.1016/j.apcata.2004.05.039.

[7] Costantino, U., Curini, M., Montanari, F., Nocchetti, M., Rosati, O. (2003). Hydrotalcitelike Compounds as Catalysts in Liquid Phase Organic Synthesis: I. Knoevenagel Condensation Promoted by $Ni_{0.73}Al_{0.27}(OH)_2](CO_3)_{0.135}$. *J. Mol. Catal. A: Chem.*, 195, 245–252. DOI: 10.1016/S1381-1169(02)00580-0.

[8] Choudary, B.M., Madhi, S., Chowdari, N.S., Kantam, M.L., Sreedhar, B. (2002). Layered Double Hydroxide Supported Nanopalladium Catalyst for Heck-, Suzuki-, Sonogashira-, and Stille-Type Coupling Reactions of Chloroarenes. *J. Am. Chem. Soc.*, 124, 14127–14136. DOI: 10.1021/ja026975w.

[9] Rives, V., Prieto, O., Dubey, A., Kannan, S. (2003). Synergistic Effect in the Hydroxylation of Phenol over CoNiAl Ternary Hydrotalcites. *J. Catal.*, 220, 161–171. DOI: 10.1016/S0021-9517(03)00245-8.

[10] Bish, D.L. (1980). Anion Exchange in Takovite: Applications to Other Hydroxide Minerals. *Bull. Mineral*, 103, 170–175. DOI: 10.3406/bulmi.1980.7392.

[11] Comelli, N.A., Ruiz M.L., Aparicio, M.S.L., Merino N.A., Cecilia, J.A., Rodríguez Castellón, E., Lick, I.D., Ponzi M.I. (2018). Influence of the synthetic conditions on the composition, morphology of CuMgAl hydrotalcites and their use as catalytic precursor in Diesel soot combustion reactions. *Applied Clay Science*, 157, 148-157. DOI: 10.1016/j.clay.2018.02.039.

[12] Corma, A., Palomares, A.E., Rey, F., Marquez, F. (1997). Simultaneous Catalytic Removal of SOx and NOx with Hydrotalcite Derived Mixed Oxides Containing Copper, and Their Possibilities to be used in FCC Units. *J. Catal.*, 170, 140–149. DOI: 10.1006/jcat.1997.1750.

[13] Palomares, A.E., Lopez-Nieto, J.M., Lazaro, F.J., Lopez, A., Corma, A. (1999). Reactivity in the Removal of SO_2 and NOx on Co/Mg/Al Mixed Oxides Derived from Hydrotalcites. *Appl. Catal. B Environ.*, 20, 257–266. DOI: 10.1016/S0926-3373(98)00121-0.

[14] Huang, X., Yang, X., Li, G., I. Ezeh, C., Sun, C., Snape, C. (2019). Hybrid Two-step Preparation of Nanosized MgAl Layered Double Hydroxides for CO_2 Adsorption. *Infotech*, Chapter, 10, 1-21. DOI: 10.5772/infotechopen.8660.

[15] Aminu, K., Nooraini, A., Mohd, H., Sharida, F.H., Samer, A. (2014). Toxicity and Metabolism of Layered Double Hydroxide Intercalated with Levodopa in a Parkinson's Disease Model. *Int. J. Mol. Sci.*, 15, 5916–5927. DOI: 10.3390/ijms15045916.

[16] Kim, H.J., Lee, G.J., Choi, A.J., Kim, T.H., Kim, T.I., Oh, J.M. (2018). Layered double hydroxide nanomaterials encapsulating angelica gigas nakai extract for potential anticancer nanomedicine. *Front. Pharmacol.*, 9, 723. DOI: 10.3389/fphar.2018.00723.

[17] Qin-Zheng, Y., Ying-Yue, C., Hua-Zhang, Z. (2013). Preparation and antibacterial activity of lysozyme and layered double hydroxide nanocomposites. *Water Res.* 1; 47(17), 6712-8. DOI: 10.1016/j.watres.2013.09.002.

[18] Lagnamayee, M., Dhananjaya, P., Kulamani, P., Javaid, Z.S. (2017). Enhanced Photocatalytic Activity of a Molybdate-Intercalated Iron-Based Layered Double Hydroxide. *Eur. J. Inorg. Chem.*, 2017, 723–733. DOI: 10.1002/ejic.201601191.

[19] Kentaro, T., Hideo, T., Kentaro, O., Takashi, S., Tetsuya, S., Tsunehiro, T. (2014). Photoactivation of Molecular Oxygen by an Iron (III) Porphyrin with a Magnesium Aluminum Layered Double Hydroxide for the Aerobic Epoxidation of Cyclohexene. *ChemCatChem*, 6, 2276–2281. DOI: 10.1002/cctc.201402131.

[20] Shirley, N., Kelly, A.D.F.C., Geani, M.U., Matilte, H., Vanessa, P., Claude, F., Fernando, W. (2014). Anionic Iron(III) Porphyrin Immobilized on/into Exfoliated Macroporous Layered Double Hydroxides as Catalyst for Oxidation Reactions. *J. Braz. Chem. Soc*., 25 (12), DOI: 10.5935/0103-5053.20140241.

[21] Xianggui, K., Jingwen, Z., Jingbin, H., Danyao, Z., Min, W., Xue, D. (2011). Fabrication of Naphthol Green B/Layered Double Hydroxide Nanosheets Ultrathin Film and Its Application in Electrocatalysis. *Electrochim. Acta*., 56, 1123–1129. DOI: 10.1016/j.electacta.2010.10.081.

[22] Hessamaddin, S., Alireza, K., Shahin, G., Mir R.M., Yasin, O. (2021). A review of status and prospects Layer double hydroxides (LDHs)-based electrochemical and optical sensing assessments for quantification and identification of heavy metals in water and environment samples. *Trends in Environmental Analytical Chemistry,* 31, e00139. DOI: 10.1016/j.teac.2021.e00139.

[23] Kiyoharu, T., Kohei, I., Takashi, K., Akira, M., Mikio, H. (2015). Development of Alkaline Fuel Cells Using Hydroxide-Ion Conductive Layered Double Hydroxides. *ECS Transactions*, 69, 17, 385-390. DOI: 10.1149/06917.0385ecst.

[24] Yu, F., Zhou, H., Huang, Y., Jingying, S., Fan, Q., Jiming, B., William, A.G., Shuo, C., Zhifeng, R. (2018). High-performance bifunctional porous non-noble metal phosphide catalyst for overall water splitting. *Nature Communications*, 9(1), 2551. DOI: 10.1038/s414167-018-04746-z

[25] Xiao, X., Huang, D., Fu, Y. Ming, W., Xingxing, J., Xiaowei, L., Lin, G., Shuanghuang, L., Mengkui, W., Chuan, Z., Yan, S. (2018). Engineering NiS/Ni2P heterostrucures for efficient electrocatalytic water splitting. *ACS Applied Materials & Interfaces*, 10 (5), 4689–4696. DOI: 10.1021/acsami.7b16430.

[26] Song, Y., Ji, K., Duan, H., Shao, M. (2021). Hydrogen production coupled with water and organic oxidation based on layered double hydroxides. *Exploration*, 1, 20210050., 1-12. DOI: 10.1002/EXP.20210050.

[27] Shalini, K., Nur Hawa, N.A., Yusran, S. (2020). Advances in Layered Double Hydroxide/Carbon Nanocomposites Containing Ni^{2+} and $Co^{2+/3+}$ for Supercapacitors. *Frontiers in Materials,* 7, 147, 1-22. DOI: 10.3389/fmats.2020.00147.

[28] Zhang, J., Wang, X., Zhan, S., Li, H., Ma, C., Qiu, Z. (2021). Synthesis of Mg/Al-LDH nanoflakes decorated magnetic mesoporous MCM-41 and its application in humic acid adsorption. *Microchemical Journal*, 162, 105839. DOI: 10.1016/j.microc.2020.105839.

[29] Fan, X., Cao, Q., Meng, F., Song, B., Bai, Z., Zhao, Y., Chen, D., Zhou, Y., Song, M. (2021). A Fenton-like system of biochar loading FeAl layered double hydroxides (FeAl-LDH@BC) / H_2O_2 for phenol removal. *Chemosphere*, 266 128992, 1-9. DOI: 10.1016/j.chemosphere.2020.128992.

[30] Xin, H., Xinhong, Q., Chenyan, H., Yawen, L. (2018). Treatment of heavy metal ions in wastewater using layered double hydroxides: A review. *Journal of Dispersion Science and Technology*, 39(6), 792-801, DOI: 10.1080/01932691.2017.1392318.

[31] Xue, B., Hui, Z., Liguang, D. (2014). Review Layered Double Hydroxide-Based Nanocarriers for Drug Delivery. *Pharmaceutics*, 6, 298-332. DOI: 10.3390/pharmaceutics6020298.

[32] Wen, J., Yang, K., Huang, J., Sun, S. (2021). Recent advances in LDH-based nanosystems for cancer therapy. *Materials and Design*, 198, 109298, DOI: 10.1016/j.matdes.2020.109298.

[33] Feng, X., Jiao, Q., Chen, W., Dang, Y., Dai, Z., Suib, S.L., Zang, J., Zhao, Y., Li, H., Feng, C. (2021). Cactus-like $NiCo_2S_4$@NiFe LDH hollow spheres as an effective oxygen bifunctional electrocatalyst in alkaline solution. *Applied Catalysis B: Environmental*, 286, 119869. DOI: 10.1016/j.apcatb.2020.119869.

[34] Bukhtiyarova, M.V. (2019). A review on effect of synthesis conditions on the formation of layered double hydroxides. *Journal of Solid State Chemistry*, 269, 494-506. DOI: 10.1016/j.jssc.2018.10.018.

[35] Zubair, M., Daud, M., McKay, G., Shehzad, F., Al-Harthi, M.A. (2017). Recent progress in layered double hydroxides (LDH)-containing hybrids as adsorbents for water remediation. *Appl. Clay Sci.*, 143, 279-292. DOI: 10.10116/j.clay.2017.04.002.

[36] Zhao, M.Q., Zhang, Q., Huang, J.Q., Wei, F. (2012). Hierarchical nanocomposites derived from nanocarbons and layered double hydroxides - properties, synthesis, and applications. *Adv. Funct. Mater.*, 22, 675–694. DOI: 10.1002/adfm.201102222.

[37] Cao, Y., Li, G., Li, X. (2016). Graphene/layered double hydroxide nanocomposite: properties, synthesis, and applications. *Chem. Eng. J.*, 292, 207–223. DOI: 10.1016/j.cej.2016.01.114.

[38] Mishra, G., Dash, B., Pandey, S. (2018). Layered double hydroxides: a brief review from fundamentals to application as evolving biomaterials. *Appl. Clay Sci.*, 153, 172–186, DOI: 10.1016/j.clay.2017.12.021.

[39] Tichit, D., Layrac, G., Gérardin, C. (2019). Synthesis of layered double hydroxides through continuous flow processes: a review. *Chem. Eng. J.*, 369, 302–332. DOI: 10.1016/j.cej.2019.03.057

[40] Forano, C., Hibino, T., Leroux, F., Taviot-Gueho, C. (2006). Layered double hydroxides. In Bergaya, F., Theng, B.K.G., Lagaly, G. (Eds.) Handbook of Clay Science vol. 1. Amsterdam: Elsevier Science Bv.

[41] Rives, V. (2001). Layered Double Hydroxides: Present and Future. New York: Nova Science Publishers, Inc.

[42] Ian, T.S. (2015). Layered Double Hydroxides (LDHs): Synthesis, Characterization and Applications. Series: Materials Science and Technologies.

[43] Costantino, U., Marmottini, F., Nocchetti, M., Vivani, R. (1998). New synthetic routes to hydrotalcite-like compounds - characterisation and properties of the obtained materials. *Eur. J. Inorg. Chem.*, 1998(10), 1439–1446. DOI: 10.1002/(SICI)1099-0682(199810)1998:103.0.CO;2-1.

[44] Conterosito, E., Beek, W.V., Palin, L., Croce, G., Perioli, L., Viterbo, D., Gatti, G., Milanesio, M. (2013). Development of a fast and clean intercalation method for organic molecules into layered double hydroxides. *Crystal growth & Design*, 13(3), 1162-1169. DOI: 10.1021/cg301505e.

[45] Jubri, Z., Hussein, M.Z., Yahaya, A., Zainal, Z. (2012). The effect of microwave-assisted synthesis on the physico-chemical properties of pamoate-intercalated layered double hydroxide. *Nanosci. Methods*, 1, 152-163. DOI: 10.1080/17458080.2011.630036.

[46] Benito, P., Guinea. I., Herrero. M., Labajos, F.M., Rives, V. (2007). Incidence of microwave hydrothermal treatments on the crystallinity properties of hydrotalcite-like compounds. *Zeitschrift fur Anorg. und Allg. Chemie.*, 633, 1815–1819. DOI: 10.1002/ZAAC.200700178.

[47] Bergadà, O., Vicente, I., Salagre, P., Cesteros, Y., Medina, F., Sueiras, J.E. (2007). Microwave effect during aging on the porosity and basic properties of hydrotalcites. *Microporous Mesoporous Mater.*, 101, 363–373. DOI: 10.1016/j.micromeso.2006.11.033.

[48] Abito, G., Bonasera, A., Prestopino, G., Orsini, A., Mattoccia, A., Martinelli, E., Pignataro, B., Medaglia, P.G. (2019). Layered Double Hydroxides: A Toolbox for Chemistry and Biology. *Crystals*, 9, 361. DOI: 10.3390/cryst9070361.

[49] Zhao, M.Q., Zhang, Q., Huang, J.Q., Wei, F. (2012). Hierarchical nanocomposites derived from nanocarbons and layered double hydroxides-properties, synthesis, and applications. *Adv. Funct. Mater.*, 22, 675–694. DOI: 10.1002/adfm.201102222.

[50] Zhen, L., Zhaoling, M., Yanyong, W., Ru, C., Zhenjun, W., Shuangyin. W. (2018). LDHs derived nanoparticle-stacked metal nitride as interlayer for long-life lithium sulfur batteries. *Science Bulletin*, 63, 3, 169-175. DOI: 10.1016/j.scib.2017.12.018.

[51] Zexuan, Z., Peilong, L., Xin, Z., Cun, H., Yuwen, L., Bin, Y., Ning, Z., Chao, L., Jiangfeng, S., Mingcan, L. (2021). Recent Advances in Layered-Double-Hydroxides Based Noble Metal Nanoparticles Efficient Electrocatalysts. *Nanomaterials,* 11, 2644, 1-17. DOI: 10.3390/nano11102644.

[52] Newman, S.P., Jones, W. (1998). Synthesis, characterization and applications of layered double hydroxides containing organic guests. *New J. Chem.*, 22, 105–115. DOI: 10.1039/A708319J.

[53] Leroux, F., Taviot-Guého, C. (2005). Fine tuning between organic and inorganic host structure: New trends in layered double hydroxide hybrid assemblies. *J. Mater. Chem.*, 15, 3628–3642. DOI: 10.1039/B505014F.

[54] Rives, V., Ulibarri, M.A. (1999). Layered double hydroxides (LDH) intercalated with metal coordination compounds and oxometalates *Coord. Chem. Rev.*, 181, 61–120. DOI: 10.1016/S0010-8545(98)00216-1.

[55] Omwoma, S., Chen, W., Tsunashima, R., Song, Y.F. (2014). Recent advances on polyoxometalates intercalated layered double hydroxides: from synthetic approaches to functional material applications. *Coord. Chem. Rev.*, 258–259, 58–71. DOI: 10.1016/j.ccr.2013.08.039.

[56] Bouali, A.C., Serdechnova, M., Blawert, C., Tedim, J., Ferreira, M.G.S., Zheludkevich, M.L. (2020). Layered double hydroxides (LDHs) as functional materials for the corrosion protection of aluminum alloys: A review. *Applied Materials Today*, 21, 100857, 1-42. DOI: 10.1016/j.apmt.2020.100857.

[57] Iqbal, M.A., Sun, L., Barrett, A.T., Fedel, M. (2020). Review Layered Double Hydroxide Protective Films Developed on Aluminum and Aluminum Alloys: Synthetic Methods and Anti-Corrosion Mechanisms. *Coatings*, 10, 428. DOI: 10.3390/coatings10040428.

[58] Richetts, M. (2017). Characteristics, Preparation Routes and Metallurgical Applications of LDHs: An Overview. *J. Material. Sci. Eng.*, 6(6), 1-11. DOI: 10.4172/2169-0022.1000397.

[59] Ding, X., Wu, L., Chen, J., Zhang, G., Xie, Z., Sun, D., Jiang, B., Atrens, A., Pan, F. (2020). Enhanced protective nanoparticle-modified MgAl-LDHs coatings on titanium alloy. *Surface and Coatings Technology*, 404, 126449. DOI: 10.1016/j.surfcoat.2020.126449.

[60] Liu, T., Zhou, H., Zhong, G., Yan, X., Su, X., Lin, Z. (2021). Synthesis of NiFeAl LDHs from electroplating sludge and Their excellent supercapacitor performance. Journal of Hazardous Materials, 404, 124113. DOI: 10.1016/j.jhazmat.2020.124113.

[61] Sònia, A., Francesc, M., Didier, T., Javier, P. R., Johan, C.G., Jesús, E.S., Pilar, S., Yolanda, C. (2005). Aldol condensations over reconstructed Mg-Al hydrotalcites: structure-activity relationships related to the rehydration method. *Chemistry* 1(2), 728-739. DOI: 10.1002/chem.200400409.

[62] Biplab, R., Anupam, S.R., Asit, B.P., Manirul, I.S.K, Asoke, P.C. (2016). Nano-structured Magnesium Oxide as Efficient Recyclable Catalyst for Knoevenagel and Claisen-Schmidt Condensation Reactions. *Chemistry Select*. 1, 15, 4778-47784, DOI: 10.1002/slct.201600380.

[63] Chen, D., Li, Y., Zhang, J., Zhou, J., Guo, Y., Liu, H. (2012). Magnetic Fe_3O_4/ZnCr-layered double hydroxide composite with enhanced adsorption and photo catalytic activity. *Chem. Eng. J.*, 185(186), 120–126. DOI: 10.1016/j.cej.2012.01.059.

[64] Francisco, T., Castillo-Rodríguez, J.C., Tzompantzi-Flores, C., Raúl Pérez, H., Gómez, R., Santolalla-Vargas, C.E., Che-Galicia, G., Ramos-Ramírez, E. (2021). Addition of SnO_2 over an oxygen deficient zirconium oxide (ZrxOy) and its catalytic evaluation for the photodegradation of phenol in water. *Catalysis Today*, DOI : 10.1016/j.cattod.2021.07.027.

[65] Claudia, A., Reyna, N., Barrera-Diaz, C., Martínez-Miranda, V., Julia, P., Jaime, S.V. (2013). Photocatalytically enhanced Cr(VI) removal by mixed oxides derived from MeAl (Me:Mg and/or Zn) layered double hydroxides. *Applied Catalysis B: Environmental*, 140 (141), 546-551. DOI : 10.1016/j.apcatb.2013.04.053.

[66] Sheldon, R.A. (2001). van Bekkum H. (Eds.), , Ch. 7. Fine Chemicals Through Heterogeneous Catalysis. Wiley-VCH, Weinheim.

[67] Bukhtiyarova, M.V. (2019). A review on effect of synthesis conditions on the formation of layered double hydroxides. *J. Solid State Chem.*, 269, 494–506. DOI: 10.1016/j.jssc.2018.10.018.

[68] Qiong, Z., Huan, L. (2014). Mg/Al layered double hydroxides prepared by microwave-assisted co-precipitation method for the removal of bromate. *Huan Jing Ke Xue,* 35, 4, 1566-1575.

[69] Hyung Mi, L., Mi, R.K., Sang, C.L., Seung Ho, L., Kwang, J.K. (2005). Effect of Microwave Heating on the Synthesis of Layered Double Hydroxide. *Material Science Forum*. 492-493, 743-748.

[70] Choudary, B.M., Kantam, M.L., Rahman, A., Reddy, C.V., Rao, K.K. (2001). The First Example of Activation of Molecular Oxygen by Nickel in Ni-Al Hydrotalcite: A Novel Protocol for the Selective Oxidation of Alcohols. *Angew. Chem. Int. Ed.*, 40, 763-766. DOI: 10.1002/1521-3773(20010216)40:43.0.CO;2-T

[71] Choudary, B.M., Kantam, M.L., Rahman, A., Reddy, C.R.V. (2003). Selective reduction of aldehydes to alcohols by calcined Ni-Al hydrotalcite. *Journal of Molecular Catalysis A: Chemical*, 206, 145–151. DOI: 10.1016/S1381-1169(03)00413-8.

[72] Kantan, M.L., Kavita, B., Rahman, A., Sateesh, M. (1998). Mg-$AlCO_3$ Catalysed Ring Opening of Oxiranes with TMSN3. *Indian Journal of Chemistry Sect. B.* (37), 1039-1041. http://nopr.niscair.res.in/handle/123456789/56930.

[73] Kim, T.H., Lee, G.J., Kang, J.H., Kim, H.J., Kim, T.I., Oh, J.M. (2014). Anticancer Drug-Incorporated Layered Double Hydroxide Nanohybrids and Their Enhanced Anticancer Therapeutic Efficacy in Combination Cancer Treatment. *BioMed Research International*. 193401, 1-11. DOI: 10.1155/2014/193401.

[74] Hashim, N., Hussein, MZ., Isa, I.M., Kamari, A., Mohamed, A., Azmi, M., Adila, M.J., Haf sah, T. (2014). Synthesis and controlled release of cloprop herbicides from cloprop layered double hydroxide and cloprop zinc layered hydroxide nanocomposites. *Open Journal of Inorganic Chemistry*, 4(1), 1-9. DOI: 10.4236/ojic.2014.41001.

[75] Hai Nguyen, T., Chu-Ching, L., Huang-Ping, C. (2018). Amino acids-intercalated Mg/Al layered double hydroxides as dual-electronic adsorbent for effective removal of cationic and oxyanionic metal ions. *Separation and Purification Technology*. 192, 36-45. DOI: 10.1016/j.seppur.2017.09.060.

[76] Hirokazu, N., Natsuko, W., Mitsutomo, T. (2004). Intercalation of amino acids and peptides into Mg-Al layered double hydroxide by reconstruction method. *International Journal of Pharmaceutic*s. 269(2), 469-478. DOI: 10.1016/j.ijpharm.2003.09.043.

[77] Yang, Q.Z., Chang, Y.Y., Zhao, H.Z. (2013). Preparation and Antibacterial Activity of Lysozyme and Layered Double Hydroxide Nanocomposites. *Water. Res*., 47, 6712–6718. DOI: 10.1016/j.watres.2013.09.002.

[78] Rahman, A., Al-Dayeb, S.S. (2011). Structure characterization and application of Ni hydrotalcite as solid bas catalysts for organic transformations. *J. Chil. Chem. Soc*., 56(1), 598-600. DOI: 10.4067/S0717–97072011000100017.

[79] Man, P., Chang-Il, L., Young, J. S. (2009). Hybridization of the natural antibiotic, cinnamic acid, with layered double hydroxides (LDH) as green pesticide. *Environmental Science and Pollution Research*. 17(1), 203-209. DOI: 10.1007/s11356-009-0235-0.

[80] Collins, I.E., Marco, T., Xiaogang, Y., Jun, H., Cheng-Gong, S. (2018). Ultrasonic and Hydrothermal Mediated Synthesis Routes for Functionalized Mg-Al LDH: Comparison Study on Surface Morphology, Basic Site Strength, Cyclic Sorption Efficiency and Effectiveness. *Ultrasonics Sonochemistry*, 40, 341-352. DOI: 10.1016/j.ultsonch.2017.07.013.

[81] Bayu, W., Puji, K., Purbaningtias, T.E., Fatimah, I. (2015). Synthesis and Characterization of Hydrotalcite at Different Mg/Al Molar Ratios. *Procedia Chemistry*, 17, 21–26. DOI: 10.1016/j.proche.2015.12.115.

[82] Wu, L. (2017). Influence of reaction temperature on the controlled growth of Mg-Al LDH film. *Int. J. Electrochem. Sci*., 12, 6352–6364. DOI: 10.20964/2017.07.74.

[83] Zai, J.T., Liu, Y.Y., Li, X.M., Ma, Z.F., Qi, R.R., Qian, X.F. (2017). 3D hierarchical Co–Al layered double hydroxides with long-term stabilities and high rate performances in supercapacitors. *Nano-Micro Lett*., 9, 21–29. DOI: 10.1007/s40820-016-0121-5.

[84] Choudary, B.M., Kantam, M.L., Reddy, C.V., Aranganathan, S., Lakshmi, P.S., Figueras, F. (2000). Mg–Al–O–t -Bu hydrotalcite: a new and efficient heterogeneous catalyst for transesterification. *J. Molec. Catal. A*, 159, 411–416. DOI: 10.1016/S1381-1169(00)00209-0.

[85] Nishesh Gupta, K., Md, S., Kim, S., Kim, K.S. (2020). Microscopic, spectroscopic, and experimental approach towards understanding the phosphate adsorption onto Zn–Fe layered double hydroxide. *Journal of Molecular Liquids*, 297, 111935. DOI: 10.1016/j.molliq.2019.111935.

[86] Karolina, R., Matusik, J., Kuligiewicz, A., Leiviskä, T., Cempura, G. (2021). Surface chemistry and structure evaluation of Mg/Al and Mg/Fe LDH derived from magnesite and dolomite in comparison to LDH obtained from chemicals. *Applied Surface Science*, 538, 147923. DOI: 10.1016/j.apsusc.2020.147923.

[87] Fatima, Z.M, Abderrahim, K., Mohamed, A., Noureddine, B. (2017). Zn–Al layered double hydroxides intercalated with carbonate, nitrate, chloride and sulfate ions: Synthesis, characterization and dyes removal properties. *Journal of Taibah University for Science*. 11, 1, 90-100. DOI: 10.1016/j.jtusci.2015.10.007.

[88] Luíz, P.F.B., Denise, E., Luciano de, M.G, Frederico, G.P., da Costa, L.M., Tronto, J. (2018). Layered Double Hydroxides as Hosting Matrices for Storage and Slow Release of Phosphate Analyzed by Stirred-Flow Method. *Materials Research*, 21(6), 20171004. DOI: 10.1590/1980-5373-MR-2017-1004.

[89] Giphin, G., Saravana, K.M.P. (2017). Synthesizing methods of layered double hydroxides and its use in the fabrication of dye Sensitised solar cell (DSSC): A short review. *Materials Science and Engineering,* 263, 032020, 1-9. DOI: 10.1088/1757-899X/263/3/032020.

[90] Chia-Hsuan, L., Hsueh-Liang, C., Weng-Sing, H., Moo-Chin, W., Horng-Huey, K. (2017). Synthesis and optical properties of Mg-Al layered double hydroxides precursor powders. *AIP Advances*, 7, 12, 5005, 1-11. DOI: 10.1063/1.4990832.

[91] Molano-Mendoza, M., Donneys-Victoria, D., Marriaga-Cabrales, N., Angel Mueses, M., Li Puma, G., Machuca-Martínez, F. (2018). Synthesis of Mg-Al layered double hydroxides by electrocoagulation. *Methods X*, 5, 915-923. DOI: 10.1016/j.mex.2018.07.019.

[92] Marcu, I., Urdă, A., Popescu, I., Hulea, V. (2017). Layered Double Hydroxides-Based Materials as Oxidation Catalysts. In M. Putz, & M. Mirica (Ed.) Sustainable Nanosystems Development, Properties, and Applications. Hershey, PA: IGI Global. DOI: 10.4018/978-1-5225-0492-4.ch003.

[93] Carrado, K.A., Csencsits, R., Thiyagarajan, P., Seifert, S., Macha, S.M., Harwood, J.S. (2002). Crystallization and textural porosity of synthetic clay minerals. *Journal of Materials Chemistry,* 12, 3228-3237. DOI: 10.1039/b204180b.

[94] Said, A., Mohammed, N.B., Sadik, A., Hamid, Z., Omar, Q. (2020). Effect of Mg/Al molar ratio on the basicity of Mg-Al mixed oxide derived from Mg-Al hydrotalcite. *Mediterranean Journal of Chemistry*, 10, 625-633. DOI: 10.13171/mjc10602007021464sa.

[95] Hongri, S., Haohong, D., Chunping, C., Jean-Charles, B., Dermot, O.H. (2019). Bifunctional acid–base mesoporous silica@aqueous miscible organic-layered double hydroxides. *RSC Adv.*, 9, 3749-3754. DOI: 10.1039/C9RA00188C.

[96] Debecker, D.P., Gaigneaux, E.M., Busca, Guido. (2009). Exploring, Tuning, and Exploiting the Basicity of Hydrotalcites for Applications in Heterogeneous Catalysis. *Chemistry*. 15, 3920–3935. DOI: 10.1002/chem.200900060.

[97] Ibrahim, R., Lwin, Y. (2010). Adsorbents derived from Mg-Al hydrotalcite like compounds for high temperature hydrogen storage. *Journal of Applied Sciences*, 10(12), 1128-1133. DOI: 10.3923/jas.2010.1128.1133.

[98] Saikia, H., Basumatary, S. (2019). MgRuAl-layered Double Hydroxides (LDH): An Efficient Multifunctional Catalyst for Aldol Condensation and Transfer Hydrogenation Reactions. *Current Catalysis,* 4, 8. DOI: 10.2174/2211550108666190418125857.

[99] Shanshan, X., Sarayute, C., Yan, S., Shaojun, X., Yi-chi, W., Sarah, H., Yibing, M., Yilai, J., Cristina, E.S., Huanhao, C., Xiaolei, F., Christopher, H. (2020). Mechanistic study of non-thermal plasma assisted CO_2 hydrogenation over Ru supported on MgAl layered double hydroxide. *Applied Catalysis B Environmental B,* 268, 118752, DOI: 10.1016/j.apcatb.2020.118752.

[100] Ateeq, R., Al-Dayeb, S.S. (2011). Structure characterization and application of Ni hydrotalcite as solid bas catalysts for organic transformations. *J. Chil. Chem. Soc.*, 56(1), 598-600.

[101] Harding, H., Peters, A.W., Nee, J.R.D. (2001). New developments in FCC catalyst technology. *Appl. Catal. A*, 221, 389. DOI: 10.1016/S0926-860X(01)00814-6.

[102] Xavier, K.O., Sreekala, R., Rashid, K.K.A., Yusuff, K.K.M., Sen, B. (1999). Doping effects of cerium oxide on Ni/Al2O3 catalysts for methanation. *Catal. Today*, 49, 17–21. DOI: 10.1016/s0920-5861(98)00403-9.

[103] Santos, R.M.M.D., Gonçalves, R.G.L., Constantino, V.R.L., Santilli, C.V., Borges, P.D., Tronto, J., Pinto, F.G. (2017). Adsorption of Acid Yellow 42 dye on calcined layered double hydroxide: effect of time, concentration, pH and temperature. *Appl. Clay Sci.*, 140, 132–139. DOI: 10.1016/j.clay.2017.02.005.

[104] Octavian D. Pavel, Didier T, Ioan-Cezar M (2012). Acido-basic and catalytic properties of transition-metal containing Mg–Al hydrotalcites and their corresponding mixed oxides. *Applied Clay Science,* 61, 52-58. DOI: 10.1016/j.clay.2012.03.006.

[105] Fahimeh, A, Mokhtari, J., Tahoori, F. (2019). Layered double hydroxides (LDHs): As efficient heterogeneous catalyst for the cyanosilylation of aromatic aldehydes. *Phosphorus, Sulfur, and Silicon and the Related Elements*, 194 (1-2), 76–82. DOI: 10.1080/10426507.2018.1492920.

[106] Rahman, A. (2013). Structure characterization and application of Ni hydrotalcite as environmentally friendly catalysts for reductive amination of benzaldehyde. *International Journal of Engineering Sciences & Emerging Technologies*, 56(1), 598-600.

[107] Rahman, A., Pelletier, A., Mupa, M., Mahamadi, C., Musekiwa, C. (2016). Environment-Friendly Reduction of Aromatics to Alicyclic Compounds at Room Temperature Using Superactive Calcined Ni-Al Hydrotalcite Catalysts. American *Journal of Applied Chemistry*, 4(1), 18-23. DOI: 10.11648/j.ajac.20160401.14.

[108] Choudary, B.M., Someshwar, T., Reddy, C.V., Kantam, M.L., Ratnam K.J., Sivaji, L.V. (2003). The first example of bromination of aromatic compounds with unprecedented atom economy using molecular bromine. *Applied Catalysis A: General*, 251, 397–409. DOI: 10.1016/S0926-860X(03)00379-X.

[109] Palomares, A.E., Franch, C., Corma, A. (2011). A study of different supports for the catalytic reduction of nitrates from natural water with a continuous reactor. *Catal. Today*, 172 (1), 90-94. DOI: 10.1016/j.cattod.2011.05.015.

[110] Adamski, A., Gil, B., Sojka, S. (2008). Role of vanadium sites in NO and O_2 adsorption processes over VOx/CeO_2-ZrO_2 catalysts EPR and IR studies. *Catal. Today*, 137, 292-299. DOI: 10.1016/j.cattod.2008.02.002.

[111] Olena, D., Eleonora, B., Alexey, K. (2018). Propylene oxide polymerization in the presence of layered double hydroxides. *Chem. Didact. Ecol. Metrol.* 23(1-2), 137-142. DOI: 10.1515/cdem-2018-0009.

[112] Laycock, D.E., Collacott, R.J., Skelton, D.A., Tchir, M.F. (1991). Stereospecific polymerization of propylene oxide on thermally activated synthetic hydrotalcite. *Journal of Catalysis*, 2, 354-358. DOI: 10.1016/0021-9517(91)90119-O.

[113] Tengfei, L., Lin, J.W.Z., Haralampos, N.M., Yu-Fei, S. (2018). Robust and Environmentally Benign Solid Acid Intercalation Catalysts for the Aminolysis of Epoxides. *ChemCatChem*, 10, 20, 4699-4706. DOI: 10.1002/cctc.201801119.

[114] Weijie, Z., Pingping, J., Ying, W., Jian, Z., Pingbo, Z. (2016). Manganese(III) Tetraphenylporphyrin Encapsulated by Ion Modified Hexagonal Mesoporous Silica with Unexpected Enhanced Epoxidation Selectivity. *Synthesis and Reactivity in Inorganic, Metal Organic, and Nano-Metal Chemistry*, 46, 1765–1772. DOI: 10.1080/15533174.2015.1137059.

[115] Jiang, P., Chen, M., Dong, Y., Lu, Y., Ye, X., Zhang, W. (2009). Novel Two-Phase Catalysis with Organometallic Compounds for Epoxidation of Vegetable Oils by Hydrogen Peroxide. *J. Am. Oil Chem. Soc.*, 87, 83-91. DOI: 10.1007/s11746-009-1469-1.

[116] Li, X., Jiang, P., Lu, Y., Zhang, W., Dong, Y. (2012). Synthesis of Hydrotalcite-like Com ounds Intercalated by 12- Phosphorus Tungsten Heteropoly Acid and Catalytic Performance on the Epoxidation of Fatty Acid Methyl Esters. *Acta Chim. Sin.*, 70, 544. DOI: 10.6023/A1108261.

[117] Sahoo, D.P., Nayak, S., Reddy, K.H., Martha, S., Parida, K. (2018). Fabrication of a o(OH)$_2$/ZnCr LDH "p-n" Heterojunction Photocatalyst with Enhanced Separation of Charge Carriers for Efficient Visible-Light Driven H_2 and O_2 Evolution. *Inorg. Ch*em., 57(7), 3840–3854. DOI: 10.1021/acs.inorgchem.7b03213.

[118] Sahoo, M., Mansingh, S., Subudhi, S., Mohapatra, P., Parida, K.M. (2019). A plasmonic AuPd bimetallic nanoalloy decorated over a GO/LDH hybrid nanocomposite via a green synthesis route for robust Suzuki coupling reactions: a paradigm shift towards a sustainable future. *Catalysis Science and Technology*, 9, 4678– 4692. DOI: 10.1039/C9CY01085H.

[119] Sahoo, M., Singha, S., Parida, K.M. (2011). Amine functionalized layered double hydroxide: a reusable catalyst for aldol condensation. *New J. Chem.*, 35, 2503–2509. DOI: 10.1039/C1NJ20492K.

[120] Kuljiraseth, J., Wangriya, A., Malones, J.M.C., Klysubun, W., Jitkarnka, S. (2018). Synthesis and Characterization of AMO LDH-derived mixed oxides with various Mg/Al ratios as acid–basic catalysts for Esterification of benzoic acid with 2-ethylhexanol. *Applied Catalysis B: Environmental*, 243, 415-427. DOI: 10.1016/j.apcatb.2018.10.073.

[121] Walker, V., Mills, G.A. (2001). Urine 4- heptanone: a ß-oxidation product of 2- ethylhexanoic acid from plasticizers. *Clin. Chim. Acta.*, 306, 51–61. DOI: 10.1016/s0009-8981(01)00390-4.

[122] Parida, K., Das, J. (2000). Mg/Al hydrotalcites: preparation, characterization and ketonisation of acetic acid. *J. Molec. Catal. A Chem.*, 151, 185–192. DOI: 10.1016/S1381-1169(99)00240-X.

[123] Wang, Y., Yan, D., Hankari, S.E., Zou, Y., Wang, S. (2018). Recent progress on layered double hydroxides and their derivatives for electrocatalytic water splitting. *Advanced Science*, 5(8), 1800064. DOI: 10.1002/advs.201800064.

[124] Suen, N.T., Hung, S.F., Quan, Q., Zhang, N., Xu, Y.J., Chen, H.M. (2017). Electrocatalysis for the oxygen evolution reaction: recent development and future perspectives. *Chemical Society Reviews*, 46(2), 337–365. DOI: 10.1039/C6CS00328A.

[125] Wu, L., Yu, L., Xiao, X., Zhang, F., Song, S., Chen, S., Ren, Z. (2020). Review Article Recent Advances in Self-Supported Layered Double Hydroxides for Oxygen Evolution Reaction. *AAAS Research*, 2020, 3976278. DOI: 10.34133/2020/3976278.

[126] Trotochaud, L., Young, S.L., Ranney, J.K., Boettcher, S.W. (2014). Nickel-iron oxyhydroxide oxygen-evolution electrocatalysts: the role of intentional and incidental iron incorporation. *J. Am. Chem. Soc.*, 136, 6744-6753. DOI: 10.1021/ja502379c.

[127] Lyu, F., Wang, Q., Choi, S.M., Yin, Y. (2019). Noble-metal-free electrocatalysts for oxygen evolution. *Small (Weinheim an der Bergstrasse, Germany)*, 15(1), 1804201. DOI: 10.1002/smll.201804201.

[128] Vij, V., Sultan, S., Harzandi, A.M. Abhishek, M., Jitendra, N.T., Wang-Geum, L., Taeseung, Y., Kwang, S.K. (2017). Nickel-based electrocatalysts for energy-related applications: oxygen reduction, oxygen evolution, and hydrogen evolution reactions. *ACS Catalysis*, 7(10), 7196–7225. DOI: 10.1021/acscatal.7b01800.

[129] Xiao, X., Huang, D., Fu, Y. Ming, W., Xingxing, J., Xiaowei, L., Lin, G., Shuangshuang, L., Mengkui, W., Chuan, Z., Yan, S. (2018). Engineering NiS/Ni2P heterostructures for efficient electrocatalytic water splitting. *ACS Applied Materials & Interfaces*, 10(5), 4689–4696. DOI: 10.1021/acsami.7b16430.

[130] Mingfei, S., Ruikang, Z., Zhenhua, L., Min, W., David, G.E., Xue, D. (2015). Layered double hydroxides toward electrochemical energy storage and conversion: design, synthesis and applications. *Chemical Communications,* 51, 15880-15893. DOI: 10.1039/C5CC07296D.

[131] Jing, H., Xiaomin, T., Qing, D., Zhiqiang, L., Huamin, Z., Anmin, Z., Zhizhang, Y., Xianfeng, L. (2021). Layered double hydroxide membrane with high hydroxide conductivity and ion selectivity for energy storage device. *Nature Communications*, 12, 3409, 1-10. DOI: 10.1038/s41467-021-23721-9.

[132] Likius, D., Rahman, A., Zivayi, C., Uahengo, V. (2020). Recent Advances on the Use of Nickel Nano Layered Double Hydroxides as Green, and Efficient, Catalysts for Water Splitting. *Catalysis Letters*, 150, 1942–1956. DOI: 10.1007/s10562-019-03095-w.

[133] Chen, C., Li, T., Shiqian, D., Wei, C., Yanyong, W., Yuqin, Z., Shuangyin, W. (2020). Advanced Exfoliation Strategies for Layered Double Hydroxides and Applications in Energy Conversion and Storage. *Advanced Functional Materials*. 30, 14, 1909832. DOI: 10.1002/adfm.201909832.

[134] Rong, L., Yanyong, W., Dongdong, L., Yuqin, Z., Shuangyin, W. (2017). Water-Plasma-Enabled Exfoliation of Ultrathin Layered Double Hydroxide Nanosheets with Multivacancies for Water Oxidation. *Advanced Materials*, 29, 30, 1701546. DOI: 10.1002/adma.201701546.

[135] Uwasu, M., Hara, K., Yabar, H. (2014). World cement production and environmental implications. *Environ. Dev.*, 10, 36–47. DOI: 10.1016/j.envdev.2014.02.005.

[136] Kim, Y., Worrell, E. (2002). CO2 emission trends in the cement industry: An international comparison. *Mitig. Adapt. Strateg. Glob. Chang.*, 7, 115–133. DOI: 10.1023/A:1022857829028.

[137] Tuutti, K. (1982). Corrosion of Steel in Concrete, Technical Report, Cement-och Betonginst CBI Sweden, Stockholm, Sweden.

[138] Bertolini, L., Elsener, B., Pedeferri, P., Redaelli, E., Polder, R. (2013). Corrosion of Steel in Concrete Volume 392. Weinheim, Germany: Wiley-Vch.

[139] Cai, H., Liu, X. (1998). Freeze-thaw durability of concrete: Ice formation process in pores. *Cem. Concr. Res.*, 28, 1281–1287. DOI: 10.1016/S0008-8846(98)00103-3.

[140] Huovinen, S. (1990). Abrasion of Concrete by Ice in Arctic Sea Structures, Technical, Research Centre of Finland, Espoo, Finland.

[141] Jacobsen, S., Scherer, G.W., Schulson, E.M. (2015). Concrete–ice abrasion mechanics. *Cem. Concr. Res.*, 73, 79–95. DOI: 10.1016/j.cemconres.2015.01.001.

[142] Attiogbe, E.K., Rizkalla, S.H. (1988). Response of concrete to sulfuric acid attack. *ACI Mater. J.*, 85, 481–488.

[143] Yoon, S., Moon, J., Bae, S., Duan, X., Giannelis, E.P., Monteiro, P.M. (2014). Chloride adsorption by calcined layered double hydroxides in hardened Portland cement paste. *Mater. Chem. Phys.*, 15, 376–386. DOI: 10.1016/j.matchemphys.2014.02.026.

[144] Mir, Z.M., Bastos, A., Höche, D., Zheludkevich, M.L. (2020). Recent Advances on the Application of Layered Double Hydroxides in Concrete. *Materials*, 13, 1426. DOI: 10.3390/ma13061426.

[145] Zahid, M.M, Alexandre, B., Daniel, H., Mikhail, L.Z. (2020). Recent Advances on the Application of Layered Double Hydroxides in Concrete A Review, *Materials.* 13, 1426; 1-23. DOI: 10.3390/ma13061426.

[146] José Ignacio, V., Mònica, A., Marcelo, A. (2012). Layered double hydroxides (LDHs) as functional fillers in polymer composites. Advances in Polymer Nanocomposites: Types and applications 91-130, 1st, Chapter: 4, Publisher: Woodhead Publishing, Editors: Fengge Gao. DOI: 10.1533/9780857096241.1.91.

[147] Du, L.C., Qu, B.J. (2007). Effects of synthesis conditions on crystal morphological structures and thermal degradation behavior of hydrotalcites and flame retardant and mechanical properties of EVA/hydrotalcite blends. Polym. Compos., 28, 131-138. DOI: 10.1002/pc.20279.

[148] Jiao, C.M., Wang, Z.Z., Ye, Z., Hu, Y., Fan, W.C. (2006). Flame retardation of ethylene-vinyl acetate copolymer using nano magnesium hydroxide and nano hydrotalcite. *J. Fire Sci.*, 24, 47-64. DOI: 10.1177/0734904106053160.

[149] Costache, M.C., Heidecker, M.J., Manias, E., Camion, G., Frache, A., Beyer, G. (2007). The influence of carbon nanotubes, originally modified montmorillonites and layered double hydroxides on the thermal degradation and fire retardancy of polyethylene, ethylene-vinyl acetate polystyrene. *Polymer*, 48, 6532-6545. DOI: 10.1016/j.polymer.2007.08.059.

[150] Prasad, C., Tang, H., Liu, W. (2018). Magnetic Fe_3O_4 based layered double hydroxides (LDHs) nanocomposites (Fe_3O_4/LDHs): recent review of progress in synthesis, properties and applications. *Journal of Nanostructure in Chemistry*, 8, 393–412. DOI: 10.1007/s40097-018-0289-y.

[151] Daud, M., Kamal, M.S., Shehzad, F., Al-Harthi, M.A. (2016). Graphene/layered double hydroxides nanocomposites: a review of recent progress in synthesis and applications. *Carbon*, 104, 241–252. DOI: 10.1016/j.carbon.2016.03.057.

[152] Nalawade, P., Aware, B., Kadam, V.J., Hirlekar, R.S. (2009). Layered Double Hydroxides: A Review. *Journal of Scientific & Industrial Research*, 267(68), 267-272.

[153] Choy, J.H., Kwak, S.Y., Park, J.S., Jeong, Y.J. (2001). Cellular uptake behavior of [c32P] labeled ATP–LDH nanohybrids. *J. Mater. Chem.*, 11, 1671-1674. DOI: 10.1039/B008680.

[154] Umberto, C., Valeria, B., Giuliana, G., Francesca, M., Morena, N., Loredana, T., Vittoria, V. (2009). New Polymeric Composites Based on Poly(caprolactone) and Layered Double Hydroxides Containing Antimicrobial Species. *Applied Materials and Interfaces*, 1, 3, 668-677. DOI: 10.1021/am8001988.

[155] Umberto, C., Morena, N., Michele, S., Riccardo, V. (2009). Recent progress in the synthesis and application of organically modified hydrotalcites. *Z. Kristallogr*., 224, 273–281. DOI: 10.1524/zkri.2009.1153.

[156] Mardani, H.R. (2017). (Cu/Ni)–Al layered double hydroxides@Fe3O4 as efficient magnetic nano composite photo catalyst for visible light degradation of methylene blue. *Res. Chem. Intermed.*, 10, 5795–5810. DOI: 10.1007/s11164-017-2963-y.

[157] Chunming, S (2017). Environmental implications and applications of engineered nanoscale magnetite and its hybrid nanocomposites: A review of recent literature. *J. Hazard. Mater.*, 322(Pt A): 48–84. DOI: 10.1016/j.jhazmat.2016.06.060.

[158] Lu, L., Li, J., Ng, D.H., Yang, P., Song, P., Zuo, M. (2017). Synthesis of novel hierarchically porous Fe_3O_4@MgAl–LDH magnetic microspheres and its superb adsorption properties of dye from water. *J. Ind. Eng. Chem*., 46, 315–323. DOI: 10.1016/j.jiec.2016.10.045.

[159] Parida, K., Satpathy, M., Mohapatra, L. (2012). Incorporation of Fe^{3+} into Mg/Al layered double hydroxide framework effects on textural properties and photocatalytic activity for H_2 generation. *J. Mater. Chem*., 22, 7350–7357. DOI: 10.1039/C2JM15658J.

[160] Ran-ran, S., Liang-guo, Y., Kun, Y., Yuanfeng, H., Bin, D. (2015). Adsorption of Cd(II) by Mg–Al–CO3- and magnetic Fe_3O_4/Mg–Al–CO3-layered double hydroxides: Kinetic, isothermal, thermodynamic and mechanistic studies. *Journal of Hazardous Materials*, 299, 42-49. DOI: 10.1016/j.jhazmat.2015.06.003Get.

[161] Zhang, H., Zhang, G., Bi, X., Chen, X. (2013). Facile assembly of a hierarchical core@shell Fe_3O_4@CuMgAl-LDH (layered double hydroxide) magnetic nanocatalyst for the hydroxylation of phenol. *J. Mater. Chem. A*, 1, 5934–5942. DOI: 10.1039/C3TA10349H.

[162] Komarala, E.V.P., Nigam, S., Aslam, M., Bahadur, D. (2016). In-vitro evaluation of layered double hydroxide–Fe_3O_4 magnetic nanohybrids for thermo-chemotherapy. *New J. Chem.*, 40, 423–433. DO: 10.1039/C5NJ01701G.

[163] Wang, R.X., Wen, T., Wu, X.L., Xu, A.W. (2014). Highly efficient removal of humic acid from aqueous solutions by Mg/Al layered double hydroxides-Fe_3O_4 nanocomposites. *RSC Advances*, 4, 21802-21809. DOI: 10.1039/C4RA02212B.

[164] Hu, W., Wu, X., Jiao, F., Yang, W., Zhou, Y. (2016). Preparation and characterization of magnetic Fe_3O_4@sulfonated ß-cyclodextrin intercalated layered double hydroxides for methylene blue removal. *Desalination Water Treat.*, 57, 1–12. DOI: 10.1080/19443994.2016.1155173.

[165] Zhang, X., Wang, J., Li, R., Dai, Q., Gao, R., Liu, Q., Zhang, M. (2013). Preparation of Fe_3O_4@C@layered double hydroxide composite for magnetic separation of uranium. *Ind. Eng. Chem. Res*., 52, 10152–10159. DOI: 10.1021/ie3024438.

[166] Chen, D., Li, Y., Zhang, J., Zhou, J., Guo, Y., Liu, H. (2012). Magnetic Fe_3O_4/ZnCr-layered double hydroxide composite with enhanced adsorption and photo catalytic activity. *Chem. Eng. J*., 185(186): 120–126. DOI: 10.1016/j.cej.2012.01.059.

[167] Wang, X., Zhou, S., Wu, L. (2014). Fabrication of Fe^{3+} doped Mg/Al layered double hydroxides and their application in UV light shielding coatings. *J. Mater. Chem. C.*, 2, 5752–5758. DOI: 10.1039/C4TC00437J.

[168] Yan, L., Yang, K., Shan, R., Yu, H., Du, B. (2015). Calcined ZnAl- and Fe_3O_4/ZnAl layered double hydroxides for efficient removal of Cr(VI) from aqueous solution. *RSC Advances*, 5, 96495–96503. DOI: 10.1039/C5RA17058C.

[169] Pan, D., Zhang, H., Fan, T., Chen, J., Duan, X. (2011). Nearly monodispersed core–shell structural Fe_3O_4@DFUR–LDH sub micro particles for magnetically controlled drug delivery and release. *Chem. Commun*., 47, 908–910. DOI: 10.1039/C0CC01313G.

[170] Ni, J., Xue, J., Xie, L., Shen, J., He, G., Chen, H. (2018). Construction of magnetically separable NiAl LDH/Fe_3O_4-RGO nanocomposites with enhanced photocatalytic performance under visible light. *Phys. Chem. Chem. Phys.*, 20, 414–421. DOI: 10.1039/C7CP06682A.

[171] Koilraj, P., Sasaki, K. (20160. Fe_3O_4/MgAlNO_3 layered double hydroxide as a magnetically separable sorbent for the remediation of aqueous phosphate. *J. Environ. Chem. Eng.*, 4, 984–991. DOI: 10.1016/j.jece.2016/01.005.

[172] Moaser, A.G., Khoshnavazi, R. (2017). Facile synthesis and characterization of Fe_3O_4@MgAl-LDH@STPOM nanocomposite with highly enhanced and selective degradation of methylene blue. *New J. Chem*., 41, 9472–9481. DOI: 10.1039/C7NJ00792B.

[173] Mi, F., Chen, X., Ma, Y., Yin, S., Yuan, F., Zhang, H. (2011). Facile synthesis of hierarchical core–shell Fe_3O_4@MgAl–LDH@Au as magnetically recyclable catalysts for catalytic oxidation of alcohols. *Chem. Commun.*, 47, 12804–12806. DOI: 10.1039/c1cc15858a.

[174] Chen, D., Li, Y., Zhang, J., Li, W., Zhou, J., Shao, L., Qian, G. (2012). Efficient removal of dyes by a novel magnetic Fe_3O_4/ZnCr-layered double hydroxide adsorbent from heavy metal wastewater. *J. Hazard. Mater.*, 243, 152–160. DOI: 10.1016/j.jhazmat.2012.10.014.

[175] Shan, R., Yan, L., Yang, K., Yu, S., Hao, Y., Yu, H., Du, B. (2014). Magnetic Fe_3O_4/MgAlLDH composite for effective removal of three red dyes from aqueous solution. *Chem. Eng. J.*, 15, 38–46. DOI: 10.1016/j.cej.2014.04.105.

[176] Chen, X., Mi, F., Zhang, H., Zhang, H. (2012). Facile synthesis of a novel magnetic coreshell hierarchical composite submicrospheres Fe_3O_4@CuNiAl-LDH under ambient conditions. *Mater. Lett.*, 69, 48–51. DOI: 10.1016/j.matlet.2011.11.052.

[177] Wu, X.L., Wang, L., Chen, C.L., Xu, A.W., Wang, X.K. (2011). Waterdispersible magnetite-graphene-LDH composites for efficient arsenate removal. *J. Mater. Chem.*, 21, 17353–17359. DOI: 10.1039/C1JM12678D.

[178] Zhao, X., Wang, W.Y., Li, X.D., Li, S., Song, F. (2018). Core-shell structure of Fe_3O_4@MTXLDH/Au NPs for cancer therapy. *Mater. Sci. Eng. C*, 89, 422–428. DOI: 10.1016/j.msec.2018.04.024.

[179] Shao, M., Ning, F., Zhao, J., Wei, M., Evans, D.G., Duan, X. (2012). Preparation of Fe_3O_4@SiO_2@layered double hydroxide core–shell microspheres for magnetic separation of proteins. *J. Am. Chem. Soc.*, 134, 1071–1077. DOI: 10.1021/ja2086323.

[180] Magdalena, W., Małgorzata, K.K., Alina, P., Grzegorz, R., Tomasz, B. (2019). Removal of Heavy Metals and Metalloids from Water Using Drinking Water Treatment Residuals as Adsorbents: A Review. *Minerals,* 9, 487, 1-17. DOI: 10.3390/min9080487.

[181] Marcella, B., Francesco, M. (2018). Layered double hydroxides (LDHs): versatile and powerful hosts for different applications. *Journal of Analytical & Pharmaceutical Research,* 7, 1, 14-12. DOI: 10.15406/japlr.2018.07.00206.

[182] Lekbira, E.M., Mountassir, E.M., El-Mostafa, M., Claude, F., Mohammadine, E.H., Samir, B., Abdelaaziz, A.T., Salah, R. (2021). ZnCr-LDHs with dual adsorption and photocatalysis capability for the removal of acid orange 7 dye in aqueous solution. *Journal of Science: Advanced Materials and Devices*, 6, 1, 118-126. DOI: 10.1016/j.jsamd.2020.08.002.

[183] Dang, M., Hue, T.M., Trinh, D.V., Nguyen, N.K., Nguyen, T., Dung, D., Tran, D., Hoang, V., Phan, H., Huynh, C.D. (2018). Enhanced Photocatalytic Activity for Degradation of Organic Dyes Using Magnetite $CoFe_2O_4$/$BaTiO_3$ Composite. *Journal of Nanoscience and Nanotechnology*, 18, 11, 7850-7857. DOI: 10.1166/jnn.2018.15542.

[184] Osama, S., Hicham, M.K. (2020). Designing Dual-Function Nanostructures for Water Purification in Sunlight. *Appl. Sci.*, 10, 1786; 1-19. DOI: 10.3390/app10051786.

[185] Starukh, H., Levytska, S. (2019). The simultaneous anionic and cationic dyes removal with Zn Al layered double hydroxides. *Applied Clay Science*, 180(8), 105183. DOI: 10.1016/j.clay.2019.105183.

[186] Pshinko, G.N. (2013). Layered Double Hydroxides as Effective Adsorbents for U(VI) and Toxic Heavy Metals Removal from Aqueous Media. *Journal of Chemistry,* 347178, 1-9. DOI: 10.1155/2013/347178.

[187] Linghu, W.; Yang, H.; Sun, Y.; Sheng, G.; Huan, Y (2017). One–pot synthesis of LDH/GO composites as high effective adsorbent for the decontamination of U(VI). *ACS Sustain. Chem. Eng.,* 5, 5608–5616. DOI: 10.1021/acssuschemeng.7b01303.

[188] Saber, O.; Aljaafari, A.; Osama, M.; Alabdulgader, H (2018). Accelerating the Photocatalytic Degradation of Green Dye Pollutants by Using a New Coating Technique for Carbon Nanotubes with Nanolayered Structures and Nanocomposites. *Chemistry Open,* 7, 833–841. DOI: 10.1002/open.201800173.

[189] Reena, S., Neetu, G., Anurag, M., Rajiv, G. (2011). Heavy metals and living systems: An overview. *Indian J. Pharmacol.*, 43(3), 246–253. DOI: 10.4103/0253-7613.81505.

[190] Muhammad, S., Bertrand, P., Camille, D., Muhammad, N., Muhammad, A., Eric, P. (2014). Heavy-metal-induced reactive oxygen species: phytotoxicity and physicochemical changes in plants. *Rev. Environ. Contam. Toxicol.* 14, 232, 1-44. DOI: 10.1007/978-3-319-06746-9_1.

[191] Kano, N., Zhang, S. (2018). Adsorption of Heavy Metals on Layered Double Hydroxides (LDHs) Intercalated with Chelating Agents. Intech Open. DOI: 10.5772/intechopen.80865.

[192] Perez, M.R., Pavlovic, I., Barriga, C., Cornejo, J., Hermosin, M.C., Ulibarri, M.A. (2006). Uptake of Cu^{2+}, Cd^{2+} and Pb^{2+} on Zn-Al layered double hydroxide intercalated with EDTA. *Applied Clay Science*, 32(3), 245-251. DOI: 10.1016/j.clay.2006.01.008.

[193] Gasser, M.S., Aly, H.F. (2009). Kinetic and adsorption mechanism of Cu(II) and Pb(II) on prepared nanoparticle layered double hydroxide intercalated with EDTA. *Colloids and Surfaces A: Physicochemical and Engineering Aspects*, 6(1-3), 167-173. DOI: 10.1016/j.colsurfa.2008.11.047.

[194] Zahir, M.H., Irshad, K., Rahman, M.M., Shaikh, M.N., Rahman, M.M. (2021). Efficient Capture of Heavy Metal Ions and Arsenic with a CaY-Carbonate Layered Double-Hydroxide Nanosheet. *ACS Omega*, 6(35), 22909-22921. DOI: 10.1021/acsomega.1c03294.

[195] Buxbaum, G., Pfaff, G. (2005). Cadmium Pigments, Industrial Inorganic Pigments. Hoboken, New Jersey, USA: Wiley-VCH.

[196] Shan, R., Yan, L., Yang, K., Hao, Y., Du, B. (2015). Adsorption of Cd(II) by Mg–Al–CO3 and magnetic Fe_3O_4/Mg–Al–CO3-layered double hydroxides: kinetic, isothermal, thermo dynamic and mechanistic studies. *Hazard. Mater.*, 299, 42–49. DOI: 10.1016/j.jhazmat.2015.06.003.

[197] Zhang, F., Song, Y., Song, S., Zhang, R., Hou, W. (2015). Synthesis of magnetite–graphene oxide-layered double hydroxide composites and applications for the removal of Pb(II) and 2, 4-dichlorophenoxyacetic acid from aqueous solutions. *ACS Appl. Mater. Interfaces*, 7, 7251–7263. DOI: 10.1021/acsami.5b00433.

[198] Lijiao, M., Qing, W., Saiful, M.I, Yingchun, L., Shulan, M., Mercouri, G.K. (2016). Highly Selective and Efficient Removal of Heavy Metals by Layered Double Hydroxide Intercalated with the $MoS_4^{(2-)}$ Ion. *J. Am. Chem. Soc.* 138(8), 2858-2866. DOI: 10.1021/jacs.6b00110.

[199] Jawad, A., Liao, Z., Zhou, Z., Khan, A., Wang, T., Ifthikar, J., Shahzad, A., Chen, Z., Chen, Z. (2017). Fe-MoS_4: An Effective and Stable LDH-Based Adsorbent for Selective Removal of Heavy Metals. *ACS Appl. Mater. Interfaces*. 30, 9(34), 28451-28463. doi: 10.1021/acsami.7b07208.

[200] Asiabi, H., Yamini, Y., Shamsayei, M., Molaei, K., Shamsipur, M. (2018). Functionalized layered double hydroxide with nitrogen and sulfur co-decorated carbon dots for highly selective and efficient removal of soft Hg^{2+} and Ag^{+} ions. *J. Hazard. Mater.* 357, 217-225. DOI: 10.1016/j.jhazmat.2018.05.055.

[201] Yang, L., Xie, L., Chu, M., Wang, H., Yuan, M., Yu, Z., Wang, C., Yao, H., Islam, S.M., Shi, K., Yan, D., Ma, S., Kanatzidis, M.G. (2022) Mo_3S_{132}-Intercalated Layered Double Hydroxide: Highly Selective Removal of Heavy Metals and Simultaneous Reduction of Ag^{+} Ions to Metallic Ag^{0} Ribbons. *Angew. Chem. Int. Ed. Engl.,* 61(1), e202112511. DOI: 10.1002/anie.202112511.

[202] Ekubatsion, L.H., Thriveni, T., Ahn, J.W. (2021). Removal of Cd^{2+} and Pb^{2+} from Wastewater through Sequent Addition of KR-Slag, $Ca(OH)_2$ Derived from Eggshells and CO_2 Gas. *ACS Omega*, 6(42), 27600-27609. DOI: 10.1021/acsomega.1c00946.

[203] Liang, X., Hou, W., Xu, Y., Sun, G., Wang, L., Sun, Y., Qin, X. (2010). Sorption of lead ion by layered double hydroxide intercalated with diethylenetriaminepentaacetic acid. *Colloids and Surfaces A: Physicochemical and Engineering Aspects*. 366(1), 50-57. DOI: 10.1016/j.colsurfa.2010.05.012.